Article

Cell

Granzyme B Disrupts Central Metabolism and Protein Synthesis in Bacteria to Promote an Immune Cell Death Program

Graphical Abstract

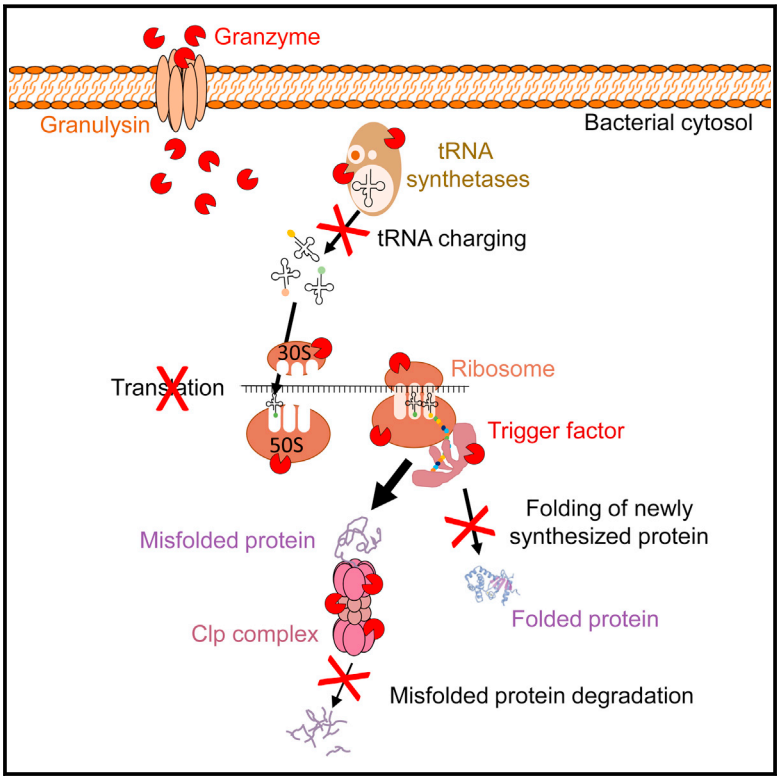

Highlights

- Granzyme B activates a multipronged program of cell death in bacteria
- Granzyme B cleaves vital biosynthetic and metabolic pathway enzymes
- 20 common orthologous groups are shared *E. coli*, listeria, and mycobacteria targets
- Like antibiotics, Granzyme B disrupts protein synthesis, folding, and degradation

Authors

Farokh Dotiwala, Sumit Sen Santara, Andres Ariel Binker-Cosen, Bo Li, Sriram Chandrasekaran, Judy Lieberman

Correspondence

fdotiwala@Wistar.org (F.D.), csriram@umich.edu (S.C.), judy.lieberman@childrens.harvard.edu (J.L.)

In Brief

Granzyme B, released by cytotoxic immune cells, causes cell death by targeting key proteostatic proteins and pathways in a range of pathogenic bacteria.

Dotiwala et al., 2017, Cell *171*, 1125–1137
November 16, 2017 © 2017 Elsevier Inc.
https://doi.org/10.1016/j.cell.2017.10.004

CellPress

Article

Cell

Granzyme B Disrupts Central Metabolism and Protein Synthesis in Bacteria to Promote an Immune Cell Death Program

Farokh Dotiwala,[1,2,6,7,8,*] Sumit Sen Santara,[1,2,7] Andres Ariel Binker-Cosen,[1,2,3,7] Bo Li,[4] Sriram Chandrasekaran,[5,8,*] and Judy Lieberman[1,2,8,9,*]

[1]Program in Cellular and Molecular Medicine, Boston Children's Hospital, Boston, MA 02115, USA
[2]Department of Pediatrics, Harvard Medical School, Boston, MA 02115, USA
[3]Department of Molecular and Cellular Biology, Harvard University, Cambridge, MA 02138, USA
[4]Program in Virology, Harvard Medical School, Boston, MA 02142, USA
[5]Department of Biomedical Engineering, University of Michigan, Ann Arbor, MI 48109, USA
[6]Vaccine Center, Wistar Institute, Philadelphia, PA 19104, USA
[7]These authors contributed equally
[8]Senior author
[9]Lead Contact
*Correspondence: fdotiwala@Wistar.org (F.D.), csriram@umich.edu (S.C.), judy.lieberman@childrens.harvard.edu (J.L.)
https://doi.org/10.1016/j.cell.2017.10.004

SUMMARY

Human cytotoxic lymphocytes kill intracellular microbes. The cytotoxic granule granzyme proteases released by cytotoxic lymphocytes trigger oxidative bacterial death by disrupting electron transport, generating superoxide anion and inactivating bacterial oxidative defenses. However, they also cause non-oxidative cell death because anaerobic bacteria are also killed. Here, we use differential proteomics to identify granzyme B substrates in three unrelated bacteria: *Escherichia coli*, *Listeria monocytogenes*, and *Mycobacteria tuberculosis*. Granzyme B cleaves a highly conserved set of proteins in all three bacteria, which function in vital biosynthetic and metabolic pathways that are critical for bacterial survival under diverse environmental conditions. Key proteins required for protein synthesis, folding, and degradation are also substrates, including multiple aminoacyl tRNA synthetases, ribosomal proteins, protein chaperones, and the Clp system. Because killer cells use a multipronged strategy to target vital pathways, bacteria may not easily become resistant to killer cell attack.

INTRODUCTION

Natural killer (NK) and cytotoxic T lymphocytes trigger programmed cell death of infected cells by releasing cytotoxic granule contents into the immune synapse formed with the target cell (Lieberman, 2012). The cytotoxic granule pore-forming protein, perforin (PFN), delivers the death-inducing granzyme (Gzm) serine proteases into the target cell, where they cleave multiple substrates to kill the target cell. These cytotoxic cells also kill intracellular bacteria and protozoa (Dotiwala et al., 2016; Walch et al., 2014). Granulysin (GNLY), another pore-forming protein in the cytotoxic granules of killer cells of most mammals, but not rodents, selectively permeabilizes microbial membranes (Stenger et al., 1998) and delivers the Gzms into intracellular microbes to cause rapid microbial death before the host cell is killed. Transgenic mice expressing *GNLY* in killer lymphocytes are better able to defend against *L. monocytogenes* (Lm), *Trypanosoma cruzi*, and *Toxoplasma gondii* infections than wild-type mice, which lack GNLY. Gzms A and B, the most abundant and best studied of the 5 human Gzms, rapidly trigger oxidative bacterial death by cleaving and disrupting electron transport chain complex I (ETC I), which generates toxic superoxide anions. At the same time, the Gzms degrade bacterial oxidative defense enzymes to disrupt the ability of bacteria to survive oxidative stress.

Aerobic bacteria begin to die within 5 min of exposure to GzmB and GNLY. However, bacteria, grown under anaerobic conditions or lacking ETC I, which do not generate reactive oxygen species (ROS) after GzmB and GNLY treatment, still die, but more slowly, within ~1 hr (Walch et al., 2014). Similarly, incubation with ROS scavengers or overexpression of oxidative defense enzymes protects bacteria from rapid Gzm-mediated death but does not prevent slower oxidation-independent death. These findings suggest that the Gzms kill bacteria by cleaving other bacterial substrates not involved in oxidoreduction reactions or oxidative defense. To uncover other bacterial cell death pathways unleashed by the Gzms, here, we used differential proteomics to identify candidate GzmB substrates in three evolutionarily diverse bacterial species, *E. coli* (Ec), Lm, and *M. tuberculosis* (MTB). We found that GzmB targets functionally related substrates in these bacteria and selectively cleaves proteins involved in critical biosynthetic and metabolic pathways. In particular, proteins needed for protein synthesis, the target of most antibiotics, were shared GzmB substrates. We biochemically validated some of these GzmB substrates and showed

that GzmB causes bacterial ribosome disassembly and blocks protein synthesis.

RESULTS

GzmB Cleaves a Conserved Core Set of Vital Proteins in *Escherichia coli*, *Listeria monocytogenes*, and *Mycobacteria tuberculosis*

We previously used 2-d IEF-SDS-PAGE differential proteomics to identify Gzm substrates in mammalian cells with high specificity (Jacquemin et al., 2014; Martinvalet et al., 2008; Rajani et al., 2012). More recently GNLY and Gzms were shown to rapidly kill Ec, Lm, and *Staphylococcus aureus* (Walch et al., 2014). Because earlier studies indicated that MTB was susceptible to high GNLY concentrations (Stenger et al., 1998), and because of the clinical importance of mycobacterial infection, we also examined whether GNLY and GzmB also efficiently kill mycobacteria, using the nonpathogenic *M. smegmatis* (Ms) strain as a model (Figure S1A). The two cytotoxic molecules at nanomolar concentrations killed Ms much more effectively than either molecule on its own. Because bacterial killing appears to be strain-independent, it is likely that killer cells are active against mycobacterial species in general, including MTB. To identify GzmB substrates in Ec, Lm, and MTB, bacterial lysates were incubated for 30 min with active or proteolytically inactive, S-A active site mutant GzmB, and the lysates were analyzed by silver staining 2-D gels. We were able to resolve most of the bacterial proteome (Ec, 2,053, Lm, 1,978, and MTB, 3,375 protein spots). Spots that disappeared in the active GzmB-treated sample were analyzed by mass spectrometry. Proteins identified by multiple peptides that migrated with the expected MW and pI of the spot were selected as potential substrates. GzmB cleaved bacterial proteins selectively. 278 candidate Ec substrates (14% of resolved spots), 163 (8% of resolved spots) in Lm, and 334 (10% of resolved spots) in MTB were identified (Table S1). Candidate substrates are shown for each bacterial species in pathway maps in Figures 1A and S1B. In addition to previously identified ETC complex I and oxidative defense enzymes (Walch et al., 2014), many putative substrates were concentrated in aerobic and anaerobic metabolism and protein, nucleotide and fatty acid biosynthetic pathways. In addition, bacterial defense pathways that cope with heat shock, DNA damage, and protein folding stress (i.e., Clp proteases, see below) were enriched in targets. The substrates also included virulence factors and other antibiotic drug targets (i.e., gyrases).

To compare the substrates across species, we used the Cluster of Orthologous Group (COG) (Galperin et al., 2015; Gil et al., 2004) mapping to find common orthologs in the GzmB targets in these 3 diverse bacterial species. The candidate substrates mapped to 251, 143, and 232 COGs in Ec, Lm, and MTB, respectively (Tatusov et al., 1997) (Figure 1B; Table S1). COGs were generated by comparing the protein sequences of complete genomes combined with careful manual curation of COG membership and functional annotation (Galperin et al., 2015). The COG database collection has 4,873 COGs corresponding to more than 1.96 million genes from 650 microbial genomes. The candidate GzmB substrate COGs significantly overlapped between species, by at least 4- to 8-fold more than was expected by chance. 53 COG proteins were common to Ec and Lm targets (p value = 10^{-35}, hypergeometric test), 79 to Ec and MTB (p value = 10^{-56}), and 40 to Lm and MTB (p value = 10^{-25}). 20 COG proteins were shared candidate substrates in all three species and 132 were shared in at least two species (p value = 10^{-33}). The 20 common COG substrates all function in protein synthesis and degradation (15) or central metabolism (5) (Figure 1C). The 15 common protein synthesis COGs included tRNA synthetases, ribosomal structural proteins, translation elongation factors, protein folding chaperones, and members of the Clp protein degradation system. The five common metabolic COG candidate substrates were glycolytic and tricarboxylic acid (TCA) cycle enzymes.

Several studies have analyzed the genomes of hundreds of bacterial species to catalog minimal sets of genes that are essential to life in diverse environments. To evaluate whether GzmB selectively targets essential genes, we compared the candidate GzmB targets with a minimal list of 206 protein-coding bacterial genes deemed essential for bacterial survival and reproduction by manual annotation of the literature (Gil et al., 2004) (Figure 1B). The common GzmB targets in all 3 bacteria were highly enriched for these proteins—12 of 20 common targets were in this core set of essential genes (p = 10^{-8}). We also compared the common GzmB targets with another core gene list, obtained from analyzing the genes of 317 bacterial species that grow under diverse conditions, which are maintained even in obligate intracellular bacteria that have much attenuated genomes (Merhej et al., 2009). Again, the common GzmB targets were highly overrepresented in this core gene set (p = 10^{-10}). Thus, GzmB selectively targets essential bacterial proteins. Consistent with these observations, the common GzmB targets were also over-represented in the genome of the predicted last universal common ancestor (LUCA) of all bacteria (p = 0.04) (Weiss et al., 2016). The genome of LUCA was inferred from phylogenetic analysis of 6.1 million bacterial protein-coding genes. LUCA is predicted to be a CO_2- and N_2-fixing anaerobe.

We next identified biological pathways that were significantly enriched in the list of 132 candidate GzmB substrate COGs common to at least 2 bacterial species using annotation from the Kyoto Encyclopedia of Genes and Genomes (KEGG) database (Table S2). We measured over-representation of these pathways among the overlapping COGs compared to the rest of the genome using the hypergeometric test. These enriched pathways encompassed a broad range of carbohydrate, fatty acid, amino acid, and nucleotide metabolic and biosynthetic processes. The most significantly enriched pathways were pyruvate metabolism (p = 10^{-7}), aminoacyl-tRNA biosynthesis (p = 3.3×10^{-6}), TCA cycle (p = 2.3×10^{-5}), and glycolysis and gluconeogenesis (p = 3.7×10^{-5}), confirming that proteins essential for glycolysis and protein synthesis were selectively targeted. Other enriched pathways were involved in glutathione metabolism (part of the oxidative defense system), DNA damage repair, and degradation of organic compounds that might be nutrients or environmental toxins. The 494 candidate GzmB substrates identified in any of the three bacterial species similarly were concentrated in the same central pathways (Figure 2; Table S3).

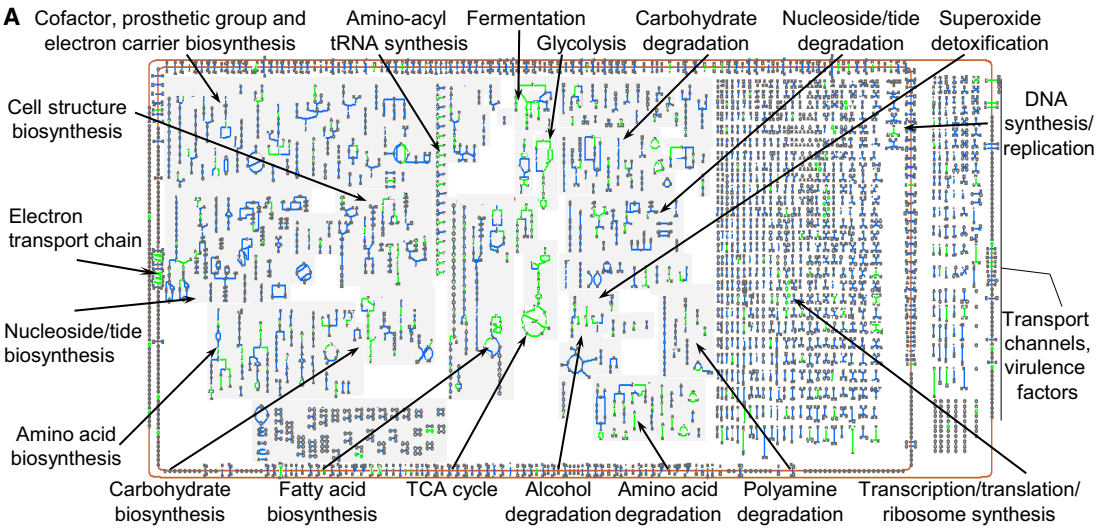

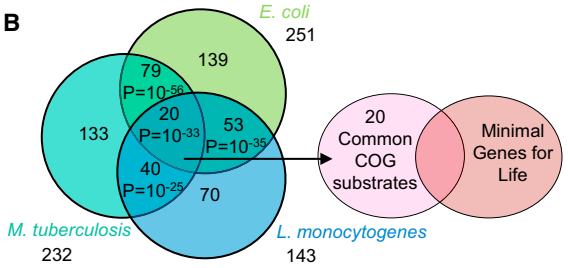

Minimal gene set	Common substrates in minimal gene set	COGs in minimal gene set	P-value
Gil et al, 2004	12/20	206	10^{-8}
Merhej et al, 2009	11/20	100	10^{-10}
Weiss et al, 2015	5/20	355	0.04

C

Protein	Function	COG ID
AlaS	Alanyl-tRNA synthetase	COG0013
LeuS	Leucyl-tRNA synthetase	COG0495
ProS	Prolyl-tRNA synthetase	COG0442
YadB	Glutamyl- and glutaminyl-tRNA synthetases	COG0008
RpsB	Ribosomal protein S2	COG0052
RpsD	Ribosomal protein S4 and related proteins	COG0522
FusA	Translation elongation factors (GTPases)	COG0480
Tsf	Translation elongation factor Ts	COG0264
Tufa	GTPases - translation elongation factors	COG0050
DnaK	Molecular chaperone	COG0443
GroEL	Chaperone GroEL (HSP60 family)	COG0459
GrpE	Molecular chaperone GrpE (heat shock protein)	COG0576
Tig	FKBP-type peptidyl-prolyl cis-trans isomerase (trigger factor)	COG0544
ClpA	ATPases with chaperone activity, ATP-binding subunit	COG0542
ClpX	ATP-dependent protease Clp, ATPase subunit	COG1219
AceF	Pyruvate/2-oxoglutarate dehydrogenase complex, dihydrolipoamide acyltransferase (E2) component	COG0508
GlmS	Glucosamine 6-phosphate synthetase, contains amidotransferase and phosphosugar isomerase domains	COG0449
GlpK	Glycerol kinase	COG0554
Lpd	Pyruvate/2-oxoglutarate dehydrogenase complex, dihydrolipoamide dehydrogenase (E3) component	COG1249
YdjI	Fructose/tagatose bisphosphate aldolase	COG0191

tRNA synthetases
Ribosome structural components
Translation elongation factors
Protein folding chaperones
Protein degradation machinery
Glycolysis and TCA

Figure 1. Comparison of Protein Targets of GzmB in *E. coli*, *L. monocytogenes*, and *M. tuberculosis*

(A) Putative Ec substrates of GzmB (green) identified by proteomics, viewed using the BioCyc Pathways tools Omics Viewer (Caspi et al., 2012). GzmB targets key metabolic and biosynthetic pathways.

(B) Venn diagram of putative GzmB substrates identified by differential proteomics. 132 COG products were shared GzmB substrates in at least 2 species and 20 were shared in all three species. The overlaps between the GzmB targets are significantly higher than expected by chance. The common GzmB targets were enriched for core COG products identified as essential for bacterial to survive in varying environments.

(C) The functions of the 20 GzmB substrates common to all 3 bacterial species. These proteins function in protein translation (tRNA synthetases, ribosomal proteins, translation elongation factors), protein folding (chaperones), protein degradation, and central metabolism (glycolysis and TCA cycle).

See also Figure S1 and Table S1.

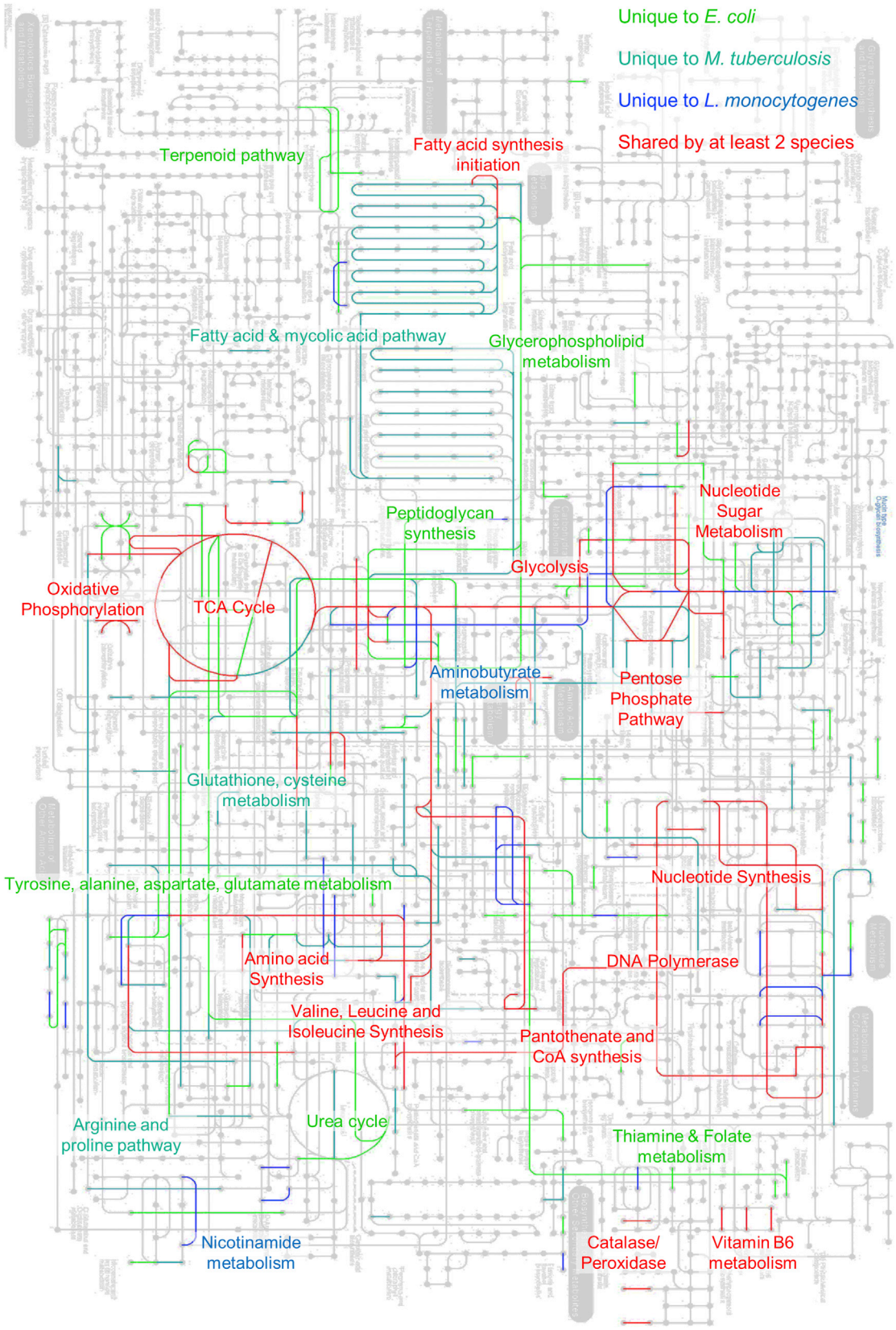

(legend on next page)

To determine if GzmB preferentially targets proteins in specific pathways over other conserved processes, we compared the composition of common orthologous proteins present in all three species with the putative GzmB targets. The common orthologs were enriched in core machinery involved in transcription, translation, and DNA replication and repair (Table S4). Although there was some overlap between the conserved pathways (Table S4) and the GzmB-targeted pathways (Tables S2 and S3), notably in ribosome components and aminoacyl-tRNA biosynthesis, the pathways over-represented in GzmB targets did not include the core pathways for DNA replication, DNA repair, or transcription. Thus, although GzmB targets vital pathways, the GzmB targets do not seem to be determined only by evolutionary conservation.

To analyze whether the GzmB targets were indeed enriched in central metabolism and protein synthesis pathways rather than being biased toward these targets because they might be more abundant, we computationally modeled the predicted targets of a "random" protease that cleaves proteins based on their abundance and conservation (as described in the STAR Methods). Our analysis revealed that the targets of GzmB differ significantly from those of a random protease (p value = 10^{-33}, t test), confirming that GzmB is not indiscriminate in its targets.

GzmB Cleaves Core Metabolic Enzymes

Because metabolic enzymes were prominent among the common GzmB targets, we analyzed the impact of inhibiting the targeted Ec metabolic enzymes using a genome-scale computational model of Ec metabolism (Orth et al., 2011). This model contains 2,251 metabolic reactions, 1,366 metabolic genes, and 1,136 metabolites. We simulated Ec metabolism in 125 growth conditions involving different carbon and nitrogen nutrient sources such as glucose, amino acids, and nucleotides, and identified metabolic genes that are essential for optimal growth (Table S5). GzmB targets included 25 key growth limiting metabolic enzymes that are required for growth in over 100 diverse growth environments (Table S6; $p = 9 \times 10^{-4}$). Thus, GzmB disrupts the ability of bacteria to survive in most metabolic conditions.

GzmB Disrupts Protein Synthesis Globally

The majority of antibiotics disrupt protein synthesis. For this reason, and because protein synthetic pathways had the most common putative GzmB targets, we focused our biochemical validation on protein synthesis. To examine the effect of GzmB on overall protein synthesis, Ec, Lm, and Ms were treated with sublytic GNLY and GzmB (200 nM), or the antibiotic translation inhibitor chloramphenicol, or transcription inhibitor rifamycin, or both. Cytotoxic lymphocyte proteins were purified as previously described (Thiery et al., 2010). GNLY was titrated for each batch to determine the sublytic concentration for each strain that causes $\leq$20% bacterial killing assessed by colony-forming unit (CFU). Protein synthesis and bacterial cell numbers were assessed by ^{35}S incorporation and CFU, respectively (Figure 3A). Experiments were performed in the presence of the superoxide scavenger Tiron to inhibit the rapid oxidative death that kills most bacteria within 5 min (Walch et al., 2014), too quickly to measure ^{35}S incorporation. New protein synthesis decreased dramatically and rapidly compared to untreated bacteria. Within 15 min of adding GzmB and GNLY and before significant bacterial death occurred, ^{35}S incorporation was reduced by approximately half, almost as much as occurred after adding rifamycin and/or chloramphenicol. Bacteria treated with GNLY and GzmB in the presence of Tiron continued to die over 4 hr until colony counts were $\sim$13% of untreated control cultures, while those treated with antibiotics remained >60% viable over 4 hr, as expected based on the known bacteriostatic properties of these antibiotics (Figure S2). To confirm that GzmB disrupts translation, we treated Ec cell lysates containing a luciferase expression plasmid with nanomolar concentrations of GzmB for 0–60 min and measured luciferase transcription and translation by luminescence (Figure 3B). Luciferase activity declined in a GzmB concentration and time-dependent manner. In the presence of 200 nM GzmB, luminescence was reduced by 60% after 15 min incubation and was undetectable above background after 60 min incubation. Thus, GzmB disrupts de novo protein synthesis in representative gram$^+$ and gram$^-$ bacteria and mycobacteria.

Because mouse GzmB has somewhat different, but overlapping, substrate activities than human GzmB (Casciola-Rosen et al., 2007; Kaiserman et al., 2006), we wanted to determine whether mouse GzmB also kills bacteria and inhibits protein synthesis. Although mouse GzmB had somewhat lower specific activity against a peptide substrate than human GzmB (Figure S3A), incubation of Ec, Lm, or Ms with mouse GzmB (200 nM) and GNLY for 20 min strongly inhibited CFU of all 3 bacteria by 80%–90%, almost as much as the same concentration of human GzmB and GNLY (Figure S3B). Moreover, GNLY and mouse or human GzmB similarly inhibited ^{35}S incorporation (Figure S3C). With either GzmB, translation was inhibited within 15 min before appreciable cell death.

To begin to examine whether the common candidate proteins important for translation identified by proteomics are bona fide targets, we expressed and purified two ribosomal protein targets, RplA and RpsD, the elongation factor FusA, and the ribosome binding ATPase/GTPase YchF, which were candidate substrates in at least two of the bacterial species we analyzed, and determined by immunoblotting with anti-His tag antibody whether they are human GzmB substrates (Figure 3C). Cleavage was assessed by progressive reduction in the full-length protein and/or detection of a cleavage band. All 4 proteins in Ec and Lm were cleaved by 100 nM GzmB, while MTB RplA, RpsD, and FusA, but not YchF, were also cleaved. It is worth noting that YchF in MTB was not a

Figure 2. Overlay of Common Protein Targets on the Universal KEGG Metabolic Map

Protein targets of GzmB in Ec, Lm, and MTB were mapped onto the universal KEGG metabolic map. Common targets shared in at least two species are shown in red. GzmB targets key metabolic pathways in energy, amino acid, lipid, nucleotide, and redox metabolism that are central to the survival of the cell.
See also Tables S2–S6.

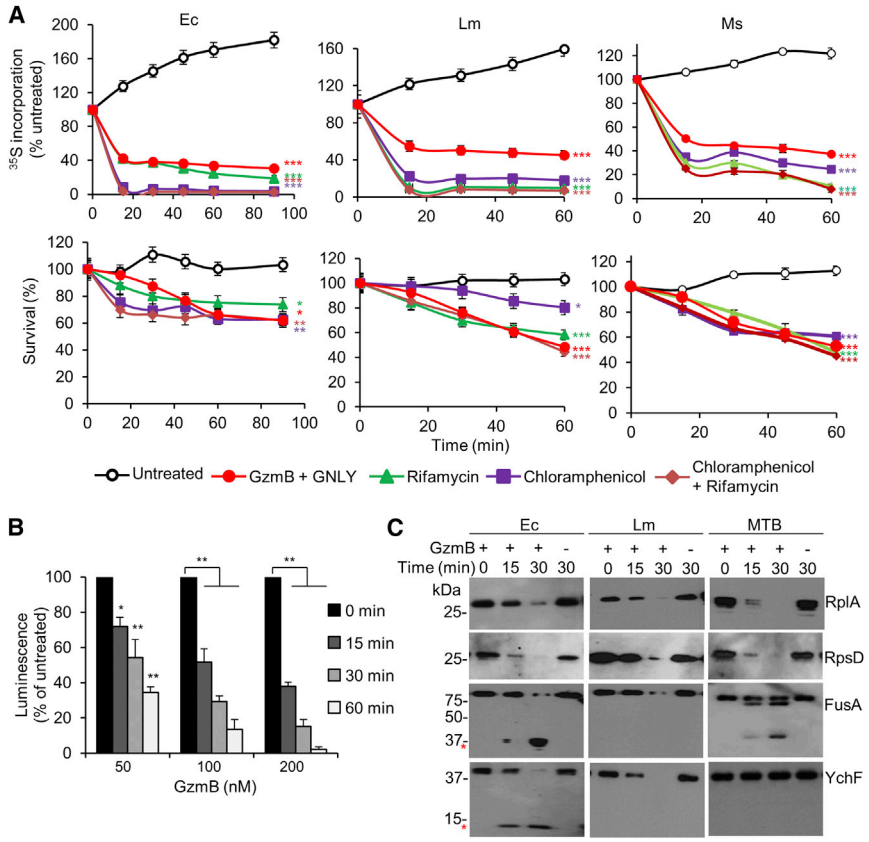

Figure 3. GzmB Disrupts Global Protein Synthesis

(A) GzmB (100 nM) and sublytic GNLY treatment of Ec (left), Lm (middle), or Ms (right) leads to rapid loss of ^{35}S incorporation (top) before loss of viability (bottom). Treatment with chloramphenicol or rifamycin were used as controls to disrupt translation elongation or transcription, respectively. The reactions were performed in the presence of an ROS scavenger to inhibit the rapid oxidative death caused by GzmB and GNLY (Walch et al., 2014). A longer time course for Ec is shown in Figure S2.

(B) In vitro transcription coupled translation of a luciferase reporter plasmid in Ec cell-free lysate treated with indicated concentrations of GzmB for indicated times, measured by luciferase activity.

(C) In vitro cleavage by 200 nM GzmB of purified recombinant Ec, Lm, and MTB ribosomal proteins and translation elongation factors. *Indicates detected cleavage products.

Mean ± SEM of three independent experiments. ***$p < 0.001$; **$p < 0.01$; *$p < 0.05$, one-way ANOVA compared to untreated bacteria (A) or to 0 min treated sample (B).

See also Figures S2, S5, and S6.

predicted GzmB substrate from the proteomics analysis. These data suggest that our proteomics predictions are reliable (11 of 11 putative substrates tested were validated) and confirm that key proteins involved in translation are GzmB substrates.

GzmB Disrupts *E. coli* Ribosomes

Because GzmB is predicted to target multiple ribosomal proteins (Figure S4), we hypothesized that GzmB would directly disrupt ribosome assembly, stability, and function. To evaluate the effect of GzmB on ribosomal structure, we treated Ec crude ribosomal fraction or purified 70S, 50S, and 30S subunits with nanomolar concentrations of human GzmB for 30 min and analyzed ribosomal integrity by density centrifugation (Figures 4A and 4B). Treatment of Ec crude ribosomal fractions or subunits reduced the abundance of intact ribosomes in a dose-dependent manner as assessed by absorbance at 260 nm without affecting ribosomal RNA (16S and 23S), measured by Bioanalyzer electropherogram (data not shown). Both human and mouse GzmB degraded Ec crude ribosomal fractions, although the mouse enzyme was less efficient (Figure S3D). We also investigated the effect of human GzmB treatment on prokaryotic polysome structure by transmission electron microscopy (TEM) (Figures 4C and 4D). When polysome fractions were purified from Ec lysates, treated with 50–200 nM human GzmB for 30 min, and imaged by negative-staining TEM, there was a dose-dependent decrease in both ribosome size and the average length of polyribosomes. We also treated purified 70S Ec ribosomes with human GzmB and used mass spectrometry to identify human GzmB cleavage products by terminal amine isotopic labeling of substrates (TAILS) (Figure 4E) (Kleifeld et al., 2011). Cleavage products of 7 ribosome proteins (RpsA, RpsC, RpsD, RplA, RplD, RplF, RplN), whose cleavage sites matched the GzmB preference for Asp at the P1 position and a neutral amino acid at the P4 position (Thornberry et al., 1997), were identified. These included 4 of the 6 ribosomal proteins identified as Ec substrates by proteomics (RpsA, RpsD, RplA, RplD) and 3 others that were not identified in Ec proteomics. Thus, GzmB directly cleaves multiple ribosomal subunits, disrupting the structure of the ribosome.

GzmB Cleaves and Inactivates Aminoacyl tRNA Synthetases

Aminoacyl tRNA synthetases (aaRS), which charge tRNAs with their respective amino acids using ATP hydrolysis for energy, were also prominent common substrates among the candidate proteomics hits (Figure S5). Twelve aaRS were identified as human GzmB targets in Ec by proteomics. To validate some of these hits, we expressed and purified tagged versions of 5 of these putative Ec substrates (GltX, HisS, LysS, MetG, TyrS) and assessed the efficiency of their cleavage (k_{CAT}/k_M) by immunoblot (Figures 5A and 5B). Human GzmB efficiently cleaved all 5 aaRS tested with k_{CAT}/k_M values of $\sim 10^4$ $M^{-1}s^{-1}$ (Figure 5B). We next assessed the effect of GzmB cleavage on aaRS function by measuring the generation of pyrophosphate, the reaction byproduct. After incubation with 100 nM human GzmB for 30 min, the ATPase activity of each of these 5 substrates was significantly reduced (Figure 5C). To verify that aaRS are cleaved

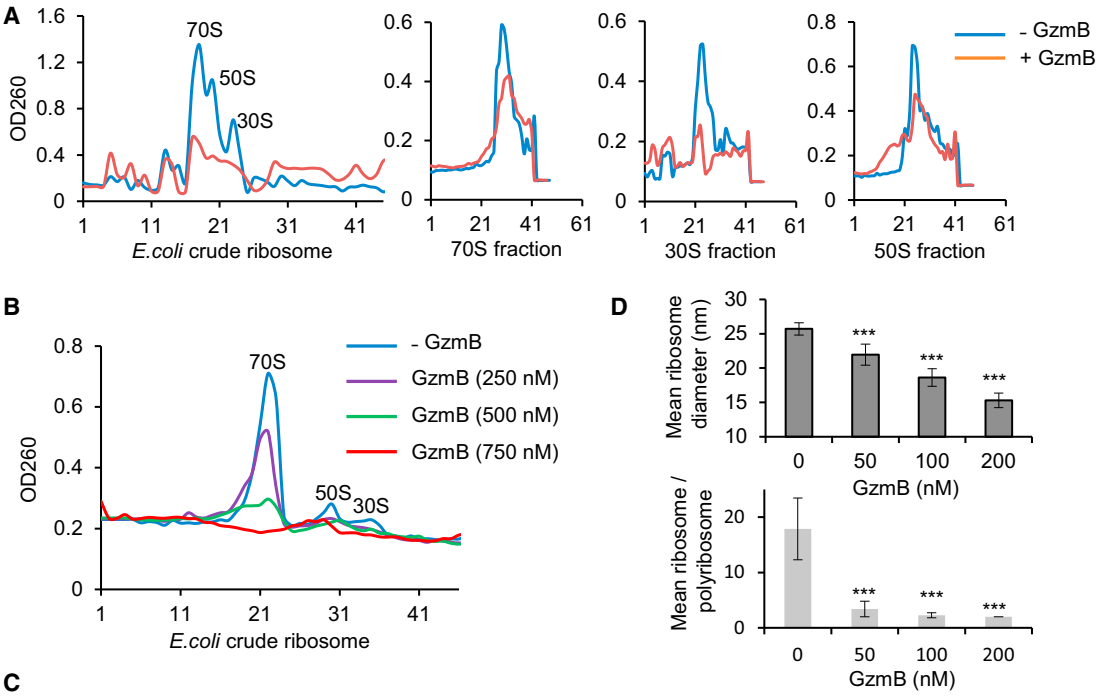

E

Protein	Detected fragments	Cut sites	Function
Rps1 (A)	D.A]VEDGFGETLLSR D.G]GIDGLVHLSDISWNVAGEEAVR.E	VALD IGLD	Protein S1,largest 30S protein
Rps3 (C)	D.F]K#VRQYLTKELAK D.I]AGVPAQINIAEVR.K	LDSD VVAD	Protein S3, binds mRNA in 70S
Rps4 (D)	D.A]GKMEGTFK#R. D.I]NEHLIVELYSK	LEVD LSAD	Protein S4, binds 16S rRNA
Rpl1 (A)	D.Q]AGLSASVN D.A]MRVVGQLGQVLGPR.G	VAVD ASPD	Protein L1, binds 23S rRNA
Rpl4 (D)	D.KVVMTADAVK	IAFD	Protein L4
Rpl6 (F)	D.LRAYRRPEPY	VAAD	Protein L6, binds to 23S rRNA
Rpl14 (N)	D.G]NACVLLNNNSEQPIGTR.I	IRFD	Protein L14, links 30S and 50S subunits

Figure 4. GzmB Degrades Bacterial Ribosomes

(A) Sucrose gradient fractionation of crude ribosomal fraction or purified 70S, 30S, or 50S ribosomes after incubation with or without 500 nM GzmB for 30 min. The absorbance at 260 nm measures RNA content of ribosomes. There was no reproducible difference in disruption of crude versus purified ribosomal fractions.

(B) Sucrose gradient fractionation of ribosomes treated with different concentrations of GzmB as in (A).

(C) Representative transmission electron microscopy negative staining images of purified Ec polysomes obtained from cell-free Ec lysates treated with 0–200 nM GzmB for 30 min (20,000× magnification). Numbers indicate mean ribosome diameter (nm). Scale bar, 100 nm.

(legend continued on next page)

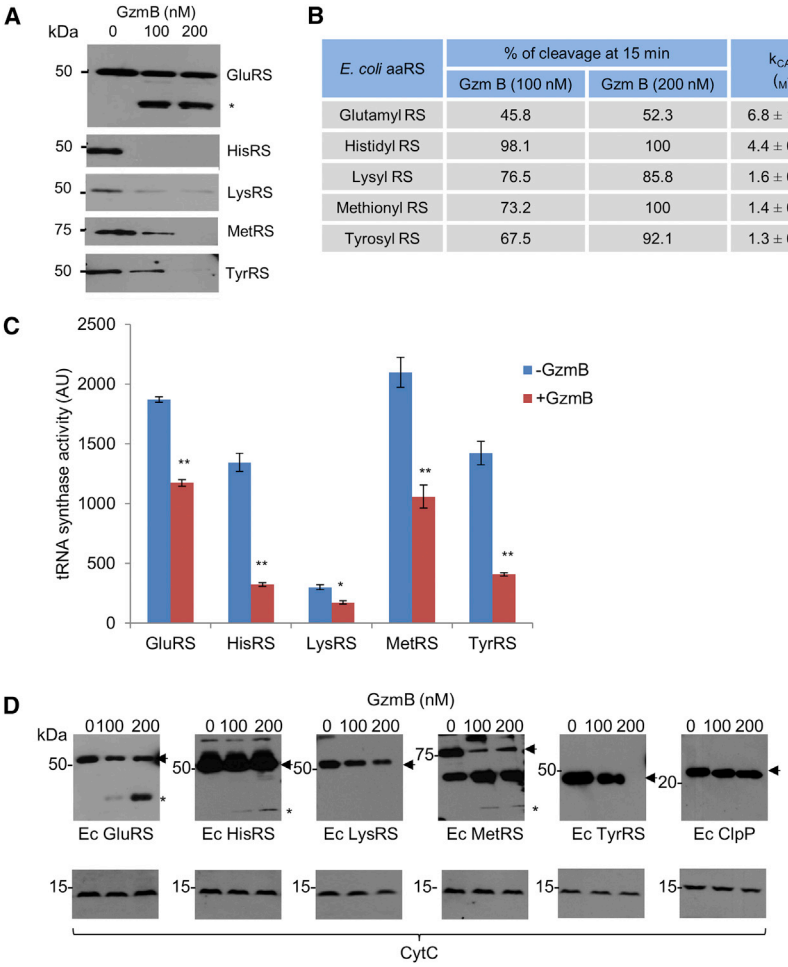

E. coli aaRS	% of cleavage at 15 min		k_{CAT}/K_M ($M^{-1}s^{-1}$)
	Gzm B (100 nM)	Gzm B (200 nM)	
Glutamyl RS	45.8	52.3	$6.8 \pm 1.7X10^3$
Histidyl RS	98.1	100	$4.4 \pm 0.4X10^4$
Lysyl RS	76.5	85.8	$1.6 \pm 0.5X10^4$
Methionyl RS	73.2	100	$1.4 \pm 0.2X10^4$
Tyrosyl RS	67.5	92.1	$1.3 \pm 0.6X10^4$

Figure 5. GzmB Cleaves and Inactivates Aminoacyl tRNA Synthetases

(A) GzmB cleaves 5 purified recombinant Ec aminoacyl tRNA synthetase (aaRS) predicted substrates. Recombinant proteins were incubated with GzmB at 37°C for 30 min and analyzed by immunoblot probed for His-tag. *Indicates detected cleavage product.

(B) GzmB catalytic activity against Ec aaRS substrates.

(C) Reduced aminoacyl synthetase activity after GzmB treatment, assessed by pyrophosphate release measured by the change in malachite green absorbance at 620–650 nm. Mean ± SEM of three independent experiments. **p < 0.01; *p < 0.05, Student's t test compared to untreated aaRS sample.

(D) Ec expressing His-tagged Ec aaRS (or Ec ClpP as an in vivo uncleaved control) (see Figure 6D) were treated with sublytic GNLY and 100–200 nM GzmB for 30 min. Immunoblots probed with anti-His tag are shown. Arrowhead, indicates full-length proteins; *, indicates cleavage fragments. Cytochrome *c* (CytC) was used as loading control.

See also Figure S4.

within intact bacteria during killer cell attack, we treated Ec expressing other His-tagged aaRS for 30 min with GNLY and nanomolar concentrations of human GzmB in the presence of 10 mM Tiron to inhibit rapid oxidative death and used anti-His tag immunoblots to assess cleavage. All 5 in vitro validated Ec aaRS substrates were also in vivo substrates. Thus, GzmB attacks multiple class I and II aaRS, which have little sequence homology, to inhibit their aaRS activity, which is essential for protein synthesis.

GzmB Disrupts Bacterial Protein Folding and Removal of Misfolded Proteins

Newly synthesized proteins, which emerge from the ribosome in an unfolded state, are protected from aggregation and degradation by the ribosome-associated chaperone trigger factor (TF), the heat shock protein DnaK, and the chaperonin GroEL (Langer et al., 1992). Lack of TF and DnaK leads to accumulation of misfolded proteins and reduced Ec viability, which is rescued by overexpression of GroEL (Genevaux et al., 2004; Mogk et al., 2011). Surprisingly, all of these key chaperones of newly synthesized proteins, TF, GroEL, and DnaK, are common putative targets of human GzmB, and other protein chaperones are also candidate substrates in some of these bacteria (Figure 1C; Table S1), suggesting that protein folding might be another process critical to protein synthesis targeted by GzmB. To begin to study the effect of GzmB on bacterial folding, we expressed and purified tagged Ec, Lm, and MTB TF and incubated them with human GzmB. All of the TFs were efficiently and rapidly degraded by nanomolar concentrations of human GzmB (Figure 6A). Next, we examined the effect of GzmB cleavage on TF folding activity using an in vitro assay that assesses refolding of guanidine HCl-denatured His-tagged recombinant GFP by measuring GFP fluorescence (Figure 6B). Pretreatment of purified recombinant Ec, Lm, and MTB TF with 100 nM human GzmB for 5–30 min decreased GFP refolding in a time-dependent manner. After 30 min of GzmB treatment, TF completely inhibited GFP refolding. Some ectopically expressed TF fragments cause protein aggregation, which inhibits even spontaneous protein refolding (Kramer et al., 2004; Merz et al.,

(D) Mean ribosome diameter (top, n = 300) and number of ribosomes/polyribosome (bottom, n = 22) measured after treatment with indicated concentrations of GzmB, as in (C). Mean ± SEM of three independent experiments. ***p < 0.001; **p < 0.01; *p < 0.05, Student's t test, compared to 0 min sample.

(E) GzmB substrates in purified Ec ribosomes and their respective cleavage sites identified by mass spectrometry using terminal amine isotopic labeling of substrate (TAILS). The cleavage sites all fit the motif characteristic of GzmB substrates. In the peptide sequences,] indicates heavy TMT-labeled N terminus, # indicates heavy TMT-labeled Lys and a period (.) indicates the cleavage site.

See also Figures S3 and S5.

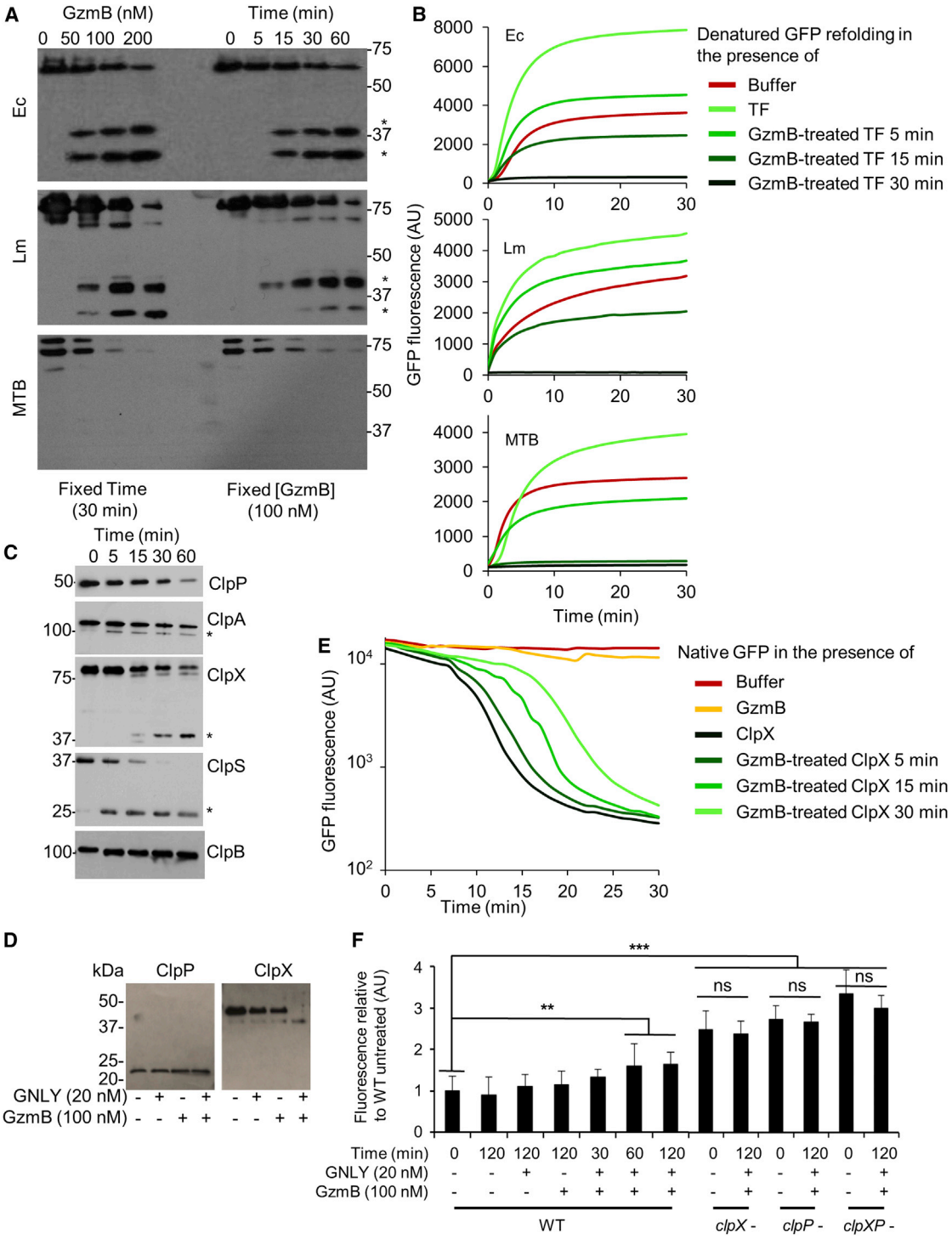

Figure 6. GzmB Disrupts the Bacterial Protein Quality-Control Machinery

(A and B) Purified recombinant Ec, Lm, and MTB trigger factor (TF) were treated with indicated concentrations of GzmB for 30 min or with 100 nM GzmB for indicated times (A) and analyzed for cleavage by anti-His immunoblot or pretreated with 100 nM GzmB for indicated times and analyzed for foldase activity on guanidinium-denatured GFP (B). In (A), * indicates cleavage product. The red curves in (B) show fluorescence of denatured GFP that was allowed to refold spontaneously as a control. AU, arbitrary units.

(C) Purified recombinant N-terminal GST-tagged Ec Clp complex proteins treated with 100 nM GzmB show time-dependent cleavage by GST immunoblot. Cleavage product indicated by *.

(legend continued on next page)

2006); we speculate that the GzmB fragments of TF also inhibited the spontaneous refolding of denatured GFP.

Cleavage of the chaperones that fold newly translated proteins is expected, even in the absence of protein aggregation caused by chaperone fragments, to increase the quantity of protein aggregates, which are toxic to bacteria. Misfolded and unfolded proteins are removed by proteolytic degradation by the Clp protease ClpP working with Clp ATPases and chaperones that unfold proteins and feed them to the protease (Gottesman et al., 1998; Kress et al., 2009). Bacteria deficient in the Clp system are impaired in handling cellular stresses and have reduced virulence. Mutation of the gene encoding the protease of the unfolded protein-degrading complex (*clpP*) is lethal for MTB (Raju et al., 2014) and reduces *S. aureus* virulence (Frees et al., 2014). Both Clp proteases and ATPases were common predicted human GzmB targets in Ec, Lm, and MTB by proteomics. Four of 5 recombinant Ec Clp proteins (the ClpP protease, ClpA and ClpX unfoldases, and the ClpS adaptor, but not ClpB, which was not identified as a candidate substrate) were cleaved by nanomolar concentrations of human GzmB (Figure 6C). Based on the extent of cleavage and cleavage kinetics, ClpS appeared to be the best substrate in the Ec Clp complex, followed by ClpA and then ClpX, while ClpP was the poorest substrate, which did not appear to decline until after ~30 min of GzmB incubation. To test whether any of the Clp proteases are cleaved in vivo in intact bacteria, we treated Ec expressing tagged ClpP or ClpX with GNLY and 100 nM human GzmB for 30 min and analyzed protein levels by immunoblot (Figure 6D). ClpX was completely degraded, but the weaker substrate ClpP did not appear to be degraded under these conditions (Figures 6C and 6D). 6 Clp subunits (B, C, E, P, P2, and X) in Lm and 3 subunits (ClpB, C1, and X) in MTB were also proteomics hits, but they were not experimentally tested as substrates (Table S1).

Based on the size of the Ec N-terminal GST-tagged 37 kDa ClpX cleavage fragment (Figure 6C), GzmB was predicted to cut ClpX after Asp144 in the AAA domain and interfere with its unfolding activity. Proteins stalled in translation are tagged with an ssrA tag, which marks the translated protein fragment for recognition by ClpX and degradation. To examine the functional consequences of GzmB cleavage of ClpX, we incubated purified GFP, bearing a C-terminal ssrA tag, with ClpX, which was pretreated or not with 100 nM GzmB for 5–30 min, and measured the decline in GFP fluorescence as a measure of ClpX-mediated unfolding (Figure 6E). ClpX completely unfolded GFP within 30 min, but GzmB on its own did not affect GFP fluorescence. However, GzmB pretreatment of ClpX reduced its unfoldase activity. When we expressed ssrA-tagged GFP in Ec, GFP fluorescence was significantly increased by treating the bacteria with GNLY and human GzmB, suggesting that GFP degradation by the Clp system was impaired (Figure 6F). Control Ec overexpressing GFP-ssrA, but deficient in ClpX and/or ClpP, had significantly higher GFP fluorescence than wild-type bacteria, and GFP fluorescence was not significantly altered by treating the Clp-deficient bacteria with GNLY and GzmB (Figure 6F). These data taken together suggest that GzmB cleavage of Clp system proteins disrupts the Clp function of removing proteins targeted for degradation.

DISCUSSION

We previously showed that killer cells use the antimicrobial cytotoxic granule protein GNLY to deliver Gzms into bacteria, which cause oxidative death by disrupting electron transport and oxidative phosphorylation, generating superoxide anion and crippling bacterial oxidative defenses. Now, we show that GzmB kills bacteria even when oxidative death is suppressed, by targeting multiple conserved biosynthetic and metabolic pathways needed for bacteria to survive in diverse environments. Key components of protein synthesis, including multiple ribosomal proteins, tRNA synthetases, protein chaperones, and the Clp system, are selectively degraded, globally disrupting the production of new proteins. Metabolic pathways critical for both oxidative metabolism and anaerobic glycolysis are predicted to be disrupted, although we did not experimentally explore the effect of GzmB on these pathways. Unlike antibiotics, which generally target a single essential protein, this bacterial immune defense utilizes a multipronged strategy to kill bacteria. We call this death "microptosis" (microbial programmed cell death), because it resembles apoptosis of eukaryotic cells, which is triggered when a cellular protease is activated that targets multiple substrates in key survival pathways.

The consequence of this multipronged strategy is that phylogenetically diverse bacteria growing under varying conditions are targeted. Developing resistance should prove difficult. Bacterial resistance could develop by bacterial strategies to cleave or inactivate the Gzms. However, human killer cells express 5 Gzm serine proteases, each with different substrate specificities (for example, GzmA cleaves after Arg or Lys, while GzmB cleaves after Asp), and each of the 3 Gzms we have looked at (A, B, M) can independently cause microptosis (Walch et al., 2014) (data not shown). The mammalian serpin granzyme inhibitors only inhibit enzymes with the same substrate specificity (Bots et al., 2006). No mammalian cell, including cancer cells, has been identified that is resistant to all the death-inducing Gzms. Similarly, it may be difficult for bacteria to develop pan-resistance to all the Gzms to subvert this immune defense. Alternate mechanisms of resistance might be alteration of bacterial membrane lipid composition to resist GNLY binding or membrane lysis or to inhibit killer cell activation or release of cytotoxic

(D) In vivo cleavage of C-terminal His-tagged ClpP or ClpX in Ec assessed 30 min after incubation with 100 nM GzmB and sublytic GNLY. Although recombinant ClpP was cleaved in vitro in (C), cleavage of ClpP was not detected within bacteria, suggesting that ClpP is not a physiologically relevant substrate.
(E) ClpX unfoldase activity on purified ssrA-tagged-GFP, measured by loss of GFP fluorescence after treatment with 100 nM GzmB.
(F) Change in in vivo ssrA-tagged GFP protein measured by GFP fluorescence in wild-type (WT) Ec treated with GNLY and/or GzmB. *ClpX*$^{-}$, *clpP*$^{-}$, or *clpXP*$^{-}$ strains were used as controls. Mean ± SEM of three independent experiments. ***p < 0.001; **p < 0.01, ns, not significant, one-way ANOVA compared to untreated WT bacteria.
In (A)–(E) representative data from three independent experiments are shown.

granules. To begin to assess whether bacteria might develop resistance, we treated Ec repeatedly for 14 passages with sublytic GNLY and GzmB and looked at whether resistance developed by measuring CFU. Yet after 14 passages, Ec did not develop resistance (Figure S6). However, it is worth looking in more detail at whether resistance develops after more prolonged exposure or in other bacterial species grown under different nutrient and environmental conditions.

Many current antibiotics inhibit different stages of bacterial protein synthesis, such as translation initiation (linezolid), aminoacyl tRNA binding (tetracyclines), peptidyl transfer (chloramphenicol, macrolides, quinupristin), ribosomal translocation (macrolides, aminoglycosides, fusidic acid), and termination (macrolides, puromycin, streptogramins). Bacterial growth is inhibited when these antibiotics bind to either the 30S subunit (aminoglycosides, tetracyclines) or the 50S subunit (chloramphenicol, macrolides, linezolid, streptogramins) of the bacterial ribosome. It is intriguing that both natural microbial products on which these antibiotics are based and immune proteases both evolved multiple strategies to disrupt protein synthesis. Drug resistance develops to these antibiotics when bacterial mutations in the ribosomal binding sites reduce antibiotic binding affinity. GzmB also disrupts bacterial pathways targeted by the next generation of antibiotics, such as mupirocin (isoleucyl t-RNA synthetase inhibitor) or acyldepsipeptide (ADEP) (ClpP activator), which are active against bacteria resistant to current antibiotics. However, these new compounds also bind to individual bacterial proteins and are also likely to induce antibiotic resistance.

Unlike the antibiotics that disrupt protein synthesis, which are mostly bacteriostatic, GzmB-mediated bacterial cell death is bactericidal, probably because it targets so many vital pathways in addition to protein synthesis. A novel strategy to develop a new type of antibiotic that could be relatively impervious to drug resistance would be to mimic granzymes by designing proteases that could enter bacteria and disrupt multiple systems in parallel. Although peptide drugs are more expensive and difficult to develop than small molecule antibiotics, the need for new strategies to overcome antibiotic drug resistance is great. The key to getting this strategy of protease antibiotics to work would be to develop feasible strategies to deliver a protease selectively into bacteria without harming mammalian cells. Some pore-forming proteins are selectively active against microbial versus mammalian membranes. For example, GNLY is inhibited by cholesterol and requires much higher concentrations to damage mammalian than bacterial membranes (Barman et al., 2006; Chung et al., 2008). Another immune pore-forming protein, gasdermin D, which is activated by innate immune sensing of invasive pathogens, damages bacterial membranes, but only damages mammalian membrane from inside cells (Liu et al., 2016).

Our experiments to test the predicted GzmB substrates in bacteria were able to confirm 20 of 21 candidate substrates (95%). These experiments independently confirmed, as GzmB substrates, 9 ribosomal proteins (in multiple bacteria), 5 tRNA synthetases in Ec, TF in Ec, Lm, and MTB, and 3 of 4 Clp proteins in Ec. This high confirmation rate, which is similar to what we previously found using the same proteomics method to identify Gzm substrates in mammalian cells, suggests that the proteomics data are reliable at identifying both individual substrates and the pathways that are disrupted. Moreover, in vitro cleavage of recombinant candidate substrates by nanomolar concentrations of recombinant GzmB strongly suggests that GzmB does not induce cell death by activating a bacterial protease, but instead directly cleaves most of the substrates we identified by analyzing the proteome of GzmB-treated whole bacterial lysates. However, the cutoffs we chose for identifying proteomics substrates were conservative and may have discarded some bona fide physiologically relevant substrates.

The Gzms, like the caspases, are selective proteases. In mammalian cells, the Gzms also do not degrade most cellular proteins. For example, even though GzmA is a tryptase, incubation of cell lysates or organelles with trypsin leads to almost complete protein digestion, but incubation with a similar concentration of GzmA only causes degradation of a small fraction of proteins. How then do the Gzms selectively target vital pathways? Although GzmB cleaves after Asp residues within preferred tetrapeptide sequences, the motif is not exact and does not predict substrate cleavage sites with specificity. The crystal structures of the granzymes have suggested that the binding pocket of the active enzymes is not very deep or specific, and substrate specificity is determined by extended binding of substrates or their binding partners to granzyme "exosites" on the surface of these very positively charged enzymes (Estébanez-Perpiña et al., 2000; Hink-Schauer et al., 2003). It is not clear whether a highly specific algorithm to predict mammalian or bacterial substrates is possible. It is surprising that the granzymes are able to "choose" essential metabolic and biosynthetic enzymes in bacteria as their substrates.

Nonetheless, it is likely that the Gzms were selected during evolution to efficiently cleave substrates that contribute effectively to their function in killing host and microbial target cells. Both Gzms and GNLY first appeared relatively recently during evolution in cartilaginous fish. Because many bacteria produce antimicrobial peptides, one wonders whether microptosis might be a more ancient pathway activated by bacterial proteases and used by aggressive bacteria to eliminate rival species in biofilms or crowded communities where nutrients are limiting. The adaptive immune system, which developed relatively late in evolution, might have hijacked a microbial pathway to control infection. Microptosis by killer cell Gzm may have similar features to the programmed cell death proposed to be induced in bacteria that are subjected to irreparable damage, for example by oxidative or DNA damage stresses or antibiotics (Bayles, 2014). The endogenous membrane pore-forming proteins ("holins") activated in bacteria by irremediable stresses may function like the BCL2 family proteins that activate mitochondrial outer membrane permeabilization in eukaryotic cells undergoing intrinsic apoptosis or the killer cell pore-forming GNLY.

Some of the pathways that the Gzms disrupt could point the way to novel targets for antibiotic drug development. Similarly, the common pathways that Gzms target in bacteria, might be disrupted by cleaving orthologous substrates in other classes of microbes, such as parasites, or even in mammalian cells.

STAR★METHODS

Detailed methods are provided in the online version of this paper and include the following:

- KEY RESOURCES TABLE
- CONTACT FOR REAGENT AND RESOURCE SHARING
- EXPERIMENTAL MODEL AND SUBJECT DETAILS
  - Bacteria
- METHODS DETAILS
  - Bacterial plasmids
  - GzmB and GNLY
  - 2D-Proteomics
  - Bioinformatics analysis
  - Metabolic network modeling
  - GzmB cleavage assay
  - In vivo global protein synthesis assay
  - In vitro transcription coupled translation assay
  - Ribosome fractionation and treatment
  - Transmission electron microscopy
  - Ribosome substrate identification by tandem mass spectrometry
  - tRNA synthetase activity assay
  - ClpX unfoldase activity assay
  - In vivo Clp activity assay
  - GFP refolding by Trigger Factor
  - Bacterial resistance assay
  - Statistical Analysis

SUPPLEMENTAL INFORMATION

Supplemental Information includes six figures and six tables and can be found with this article online at https://doi.org/10.1016/j.cell.2017.10.004.

AUTHOR CONTRIBUTIONS

F.D., S.S.S., A.A.B.-C., and J.L. designed the experiments and analyzed the data. F.D., S.S.S., A.A.B.-C., and B.L. performed experiments. S.C. performed bioinformatics analysis. F.D., S.C., and J.L. wrote the manuscript.

ACKNOWLEDGMENTS

We thank Tania Baker (MIT, Cambridge) for Ec *clpX*- strain and for the ssrA-GFP plasmid and Alfred Goldberg (HMS, Boston) for Ec *clpP*- and *clpXP*- strains and helpful discussions. We thank Maria Ericsson (HMS) for technical help with TEM and Ross Tomaino of the Taplin Mass Spectrometry Facility (HMS) for help with mass spectrometry. This work was supported by NIH RO1 AI23265 (J.L.) and T32 HL066987 (F.D.) and the Harvard Society of Fellows (S.C.).

Received: May 1, 2017
Revised: August 23, 2017
Accepted: September 30, 2017
Published: October 26, 2017

REFERENCES

Barman, H., Walch, M., Latinovic-Golic, S., Dumrese, C., Dolder, M., Groscurth, P., and Ziegler, U. (2006). Cholesterol in negatively charged lipid bilayers modulates the effect of the antimicrobial protein granulysin. J. Membr. Biol. *212*, 29–39.

Bayles, K.W. (2014). Bacterial programmed cell death: making sense of a paradox. Nat. Rev. Microbiol. *12*, 63–69.

Bots, M., VAN Bostelen, L., Rademaker, M.T., Offringa, R., and Medema, J.P. (2006). Serpins prevent granzyme-induced death in a species-specific manner. Immunol. Cell Biol. *84*, 79–86.

Casciola-Rosen, L., Garcia-Calvo, M., Bull, H.G., Becker, J.W., Hines, T., Thornberry, N.A., and Rosen, A. (2007). Mouse and human granzyme B have distinct tetrapeptide specificities and abilities to recruit the bid pathway. J. Biol. Chem. *282*, 4545–4552.

Caspi, R., Altman, T., Dreher, K., Fulcher, C.A., Subhraveti, P., Keseler, I.M., Kothari, A., Krummenacker, M., Latendresse, M., Mueller, L.A., et al. (2012). The MetaCyc database of metabolic pathways and enzymes and the BioCyc collection of pathway/genome databases. Nucleic Acids Res. *40*, D742–D753.

Cestari, I., and Stuart, K. (2013). A spectrophotometric assay for quantitative measurement of aminoacyl-tRNA synthetase activity. J. Biomol. Screen. *18*, 490–497.

Chandrasekaran, S., and Price, N.D. (2010). Probabilistic integrative modeling of genome-scale metabolic and regulatory networks in Escherichia coli and Mycobacterium tuberculosis. Proc. Natl. Acad. Sci. USA *107*, 17845–17850.

Chung, W.H., Hung, S.I., Yang, J.Y., Su, S.C., Huang, S.P., Wei, C.Y., Chin, S.W., Chiou, C.C., Chu, S.C., Ho, H.C., et al. (2008). Granulysin is a key mediator for disseminated keratinocyte death in Stevens-Johnson syndrome and toxic epidermal necrolysis. Nat. Med. *14*, 1343–1350.

Dehal, P.S., Joachimiak, M.P., Price, M.N., Bates, J.T., Baumohl, J.K., Chivian, D., Friedland, G.D., Huang, K.H., Keller, K., Novichkov, P.S., et al. (2010). MicrobesOnline: an integrated portal for comparative and functional genomics. Nucleic Acids Res. *38*, D396–D400.

Dotiwala, F., Fellay, I., Filgueira, L., Martinvalet, D., Lieberman, J., and Walch, M. (2015). A high yield and cost-efficient expression system of human granzymes in mammalian cells. J. Vis. Exp., e52911.

Dotiwala, F., Mulik, S., Polidoro, R.B., Ansara, J.A., Burleigh, B.A., Walch, M., Gazzinelli, R.T., and Lieberman, J. (2016). Killer lymphocytes use granulysin, perforin and granzymes to kill intracellular parasites. Nat. Med. *22*, 210–216.

Estébanez-Perpiña, E., Fuentes-Prior, P., Belorgey, D., Braun, M., Kiefersauer, R., Maskos, K., Huber, R., Rubin, H., and Bode, W. (2000). Crystal structure of the caspase activator human granzyme B, a proteinase highly specific for an Asp-P1 residue. Biol. Chem. *381*, 1203–1214.

Frees, D., Gerth, U., and Ingmer, H. (2014). Clp chaperones and proteases are central in stress survival, virulence and antibiotic resistance of Staphylococcus aureus. Int. J. Med. Microbiol. *304*, 142–149.

Galperin, M.Y., Makarova, K.S., Wolf, Y.I., and Koonin, E.V. (2015). Expanded microbial genome coverage and improved protein family annotation in the COG database. Nucleic Acids Res. *43*, D261–D269.

Genevaux, P., Keppel, F., Schwager, F., Langendijk-Genevaux, P.S., Hartl, F.U., and Georgopoulos, C. (2004). In vivo analysis of the overlapping functions of DnaK and trigger factor. EMBO Rep. *5*, 195–200.

Gil, R., Silva, F.J., Peretó, J., and Moya, A. (2004). Determination of the core of a minimal bacterial gene set. Microbiol. Mol. Biol. Rev. *68*, 518–537.

Gottesman, S., Roche, E., Zhou, Y., and Sauer, R.T. (1998). The ClpXP and ClpAP proteases degrade proteins with carboxy-terminal peptide tails added by the SsrA-tagging system. Genes Dev. *12*, 1338–1347.

Hink-Schauer, C., Estébanez-Perpiñá, E., Kurschus, F.C., Bode, W., and Jenne, D.E. (2003). Crystal structure of the apoptosis-inducing human granzyme A dimer. Nat. Struct. Biol. *10*, 535–540.

Jacquemin, G., Margiotta, D., Kasahara, A., Bassay, E.Y., Walch, M., Thiery, J., Lieberman, J., and Martinvalet, D. (2014). Granzyme B-induced mitochondrial ROS are required for apoptosis. Cell Death Differ. *22*, 862–874.

Kaiserman, D., Bird, C.H., Sun, J., Matthews, A., Ung, K., Whisstock, J.C., Thompson, P.E., Trapani, J.A., and Bird, P.I. (2006). The major human and mouse granzymes are structurally and functionally divergent. J. Cell Biol. *175*, 619–630.

Kanehisa, M., Goto, S., Sato, Y., Kawashima, M., Furumichi, M., and Tanabe, M. (2014). Data, information, knowledge and principle: back to metabolism in KEGG. Nucleic Acids Res. *42*, D199–D205.

Kleifeld, O., Doucet, A., Prudova, A., auf dem Keller, U., Gioia, M., Kizhakkedathu, J.N., and Overall, C.M. (2011). Identifying and quantifying proteolytic events and the natural N terminome by terminal amine isotopic labeling of substrates. Nat. Protoc. *6*, 1578–1611.

Kramer, G., Rutkowska, A., Wegrzyn, R.D., Patzelt, H., Kurz, T.A., Merz, F., Rauch, T., Vorderwülbecke, S., Deuerling, E., and Bukau, B. (2004). Functional dissection of Escherichia coli trigger factor: unraveling the function of individual domains. J. Bacteriol. *186*, 3777–3784.

Kress, W., Maglica, Z., and Weber-Ban, E. (2009). Clp chaperone-proteases: structure and function. Res. Microbiol. *160*, 618–628.

Langer, T., Lu, C., Echols, H., Flanagan, J., Hayer, M.K., and Hartl, F.U. (1992). Successive action of DnaK, DnaJ and GroEL along the pathway of chaperone-mediated protein folding. Nature *356*, 683–689.

Lieberman, J. (2012). Cell-mediated cytotoxicity. In Fundamental Immunology, W. Paul, ed. (Lippincott, Williams & Wilkins).

Liu, X., Zhang, Z., Ruan, J., Pan, Y., Magupalli, V.G., Wu, H., and Lieberman, J. (2016). Inflammasome-activated gasdermin D causes pyroptosis by forming membrane pores. Nature *535*, 153–158.

Martinvalet, D., Dykxhoorn, D.M., Ferrini, R., and Lieberman, J. (2008). Granzyme A cleaves a mitochondrial complex I protein to initiate caspase-independent cell death. Cell *133*, 681–692.

Merhej, V., Royer-Carenzi, M., Pontarotti, P., and Raoult, D. (2009). Massive comparative genomic analysis reveals convergent evolution of specialized bacteria. Biol. Direct *4*, 13.

Merz, F., Hoffmann, A., Rutkowska, A., Zachmann-Brand, B., Bukau, B., and Deuerling, E. (2006). The C-terminal domain of Escherichia coli trigger factor represents the central module of its chaperone activity. J. Biol. Chem. *281*, 31963–31971.

Mogk, A., Huber, D., and Bukau, B. (2011). Integrating protein homeostasis strategies in prokaryotes. Cold Spring Harb. Perspect. Biol. *3*, a004366.

Orth, J.D., Thiele, I., and Palsson, B.O. (2010). What is flux balance analysis? Nat. Biotechnol. *28*, 245–248.

Orth, J.D., Conrad, T.M., Na, J., Lerman, J.A., Nam, H., Feist, A.M., and Palsson, B.O. (2011). A comprehensive genome-scale reconstruction of Escherichia coli metabolism–2011. Mol. Syst. Biol. *7*, 535.

Rajani, D.K., Walch, M., Martinvalet, D., Thomas, M.P., and Lieberman, J. (2012). Alterations in RNA processing during immune-mediated programmed cell death. Proc. Natl. Acad. Sci. USA *109*, 8688–8693.

Raju, R.M., Jedrychowski, M.P., Wei, J.R., Pinkham, J.T., Park, A.S., O'Brien, K., Rehren, G., Schnappinger, D., Gygi, S.P., and Rubin, E.J. (2014). Post-translational regulation via Clp protease is critical for survival of Mycobacterium tuberculosis. PLoS Pathog. *10*, e1003994.

Rivera, M.C., Maguire, B., and Lake, J.A. (2015). Isolation of ribosomes and polysomes. Cold Spring Harb. Protoc. *2015*, 293–299.

Singh, S.K., Grimaud, R., Hoskins, J.R., Wickner, S., and Maurizi, M.R. (2000). Unfolding and internalization of proteins by the ATP-dependent proteases ClpXP and ClpAP. Proc. Natl. Acad. Sci. USA *97*, 8898–8903.

Stenger, S., Hanson, D.A., Teitelbaum, R., Dewan, P., Niazi, K.R., Froelich, C.J., Ganz, T., Thoma-Uszynski, S., Melián, A., Bogdan, C., et al. (1998). An antimicrobial activity of cytolytic T cells mediated by granulysin. Science *282*, 121–125.

Tatusov, R.L., Koonin, E.V., and Lipman, D.J. (1997). A genomic perspective on protein families. Science *278*, 631–637.

Thiery, J., Walch, M., Jensen, D.K., Martinvalet, D., and Lieberman, J. (2010). Isolation of cytotoxic T cell and NK granules and purification of their effector proteins. Curr. Protoc. Cell Biol. *Chapter 3*, Unit 3.37.

Thompson, A., Schäfer, J., Kuhn, K., Kienle, S., Schwarz, J., Schmidt, G., Neumann, T., Johnstone, R., Mohammed, A.K., and Hamon, C. (2003). Tandem mass tags: a novel quantification strategy for comparative analysis of complex protein mixtures by MS/MS. Anal. Chem. *75*, 1895–1904.

Thornberry, N.A., Rano, T.A., Peterson, E.P., Rasper, D.M., Timkey, T., Garcia-Calvo, M., Houtzager, V.M., Nordstrom, P.A., Roy, S., Vaillancourt, J.P., et al. (1997). A combinatorial approach defines specificities of members of the caspase family and granzyme B. Functional relationships established for key mediators of apoptosis. J. Biol. Chem. *272*, 17907–17911.

UniProt Consortium (2015). UniProt: a hub for protein information. Nucleic Acids Res. *43*, D204–D212.

Walch, M., Dotiwala, F., Mulik, S., Thiery, J., Kirchhausen, T., Clayberger, C., Krensky, A.M., Martinvalet, D., and Lieberman, J. (2014). Cytotoxic cells kill intracellular bacteria through granulysin-mediated delivery of granzymes. Cell *157*, 1309–1323.

Wang, M., Weiss, M., Simonovic, M., Haertinger, G., Schrimpf, S.P., Hengartner, M.O., and von Mering, C. (2012). PaxDb, a database of protein abundance averages across all three domains of life. Mol. Cell. Proteomics *11*, 492–500.

Weiss, M.C., Sousa, F.L., Mrnjavac, N., Neukirchen, S., Roettger, M., Nelson-Sathi, S., and Martin, W.F. (2016). The physiology and habitat of the last universal common ancestor. Nat. Microbiol. *1*, 16116.

STAR★METHODS

KEY RESOURCES TABLE

REAGENT or RESOURCE	SOURCE	IDENTIFIER
Antibodies		
Anti-His6 mouse monoclonal A	Covance	Cat.# MMS-156P
Anti-Cytochrome C rabbit polyclonal	Abcam	Cat.# ab18738; RRID: AB_444661
Bacterial and Virus Strains		
E. coli BL21DE3	NEB	N/A
L. monocytogenes 10403	Lab strain	N/A
Mycobacterium smegmatis (Trevisan) Lehmann and Neumann	ATCC	Cat.# NCTC 8159 [Cornell 3]
E. coli clpX-	Tania Baker (MIT)	N/A
E. coli clpP-	Alfred Goldberg (HMS)	N/A
E. coli clpXP-	Alfred Goldberg (HMS)	N/A
Biological Samples		
lysate from *M. tuberculosis* (MTB) H37Rv stain	BEI Resources	N/A
Chemicals, Peptides, and Recombinant Proteins		
DPBS	GIBCO	Cat.# 14190-144
LB Media	Thermo Fisher	Cat.# 12780-0
BHI Media	Thermo Fisher	Cat.# CM1135B
Middlebrook 7H10 Broth/Agar	Thermo Fisher	Cat.# R453982
Middlebrook OADC Growth Supplement	Sigma	Cat.# M0678-1VL
Ampicillin	Sigma	Cat.# 69-52-3
Kanamycin	Sigma	Cat.# 60615
Rifampicin	Sigma	Cat.# 557303
Chloramphenicol	Sigma	Cat.# C0378
Ni-NTA Superflow	QIAGEN	N/A
MicroScint-40	PerkinElmer	N/A
^{35}S methionine	PerkinElmer	N/A
Sephacryl S-500 HR	GE Lifesciences	N/A
IEF strips 3-10NL 17cm	BioRad	N/A
CHAPS	Sigma	Cat.# C9426
Urea	Sigma	Cat.# U0631
Thiourea	Sigma	Cat.# T8656
Sucrose (molecular biology grade)	Sigma	Cat.# S7903
DTT	Sigma	Cat.# D0632
Ribonucleic acid, transfer from *Escherichia coli*	Sigma	Cat.# R1753
Amino acids(Glutamic acid, Histidine, Lysine, Methionine, Tyrosine)	Sigma	Cat.# G1251, Cat.# H8000, Cat.# L5501, Cat.# M9625, Cat.# T3754
HBSS	GIBCO	N/A
iodoacetamide	BioRad	N/A
SDS	Sigma	Cat.# L3771
Malachite green solution	Echelon Biosciences	Cat.# K-1501
Inorganic pyrophosphatase	Sigma	N/A
Granzyme B	Lieberman Lab	N/A
Granulysin	Lieberman Lab	N/A
Ec/Lm/MTB RplA	Lieberman Lab	N/A

(*Continued on next page*)

Continued

REAGENT or RESOURCE	SOURCE	IDENTIFIER
Ec/Lm/MTB RpsD	Lieberman Lab	N/A
Ec/Lm/MTB FusA	Lieberman Lab	N/A
Ec/Lm/MTBYchF	Lieberman Lab	N/A
Ec/Lm/MTB Tig	Lieberman Lab	N/A
Ec ClpP	Lieberman Lab	N/A
Ec ClpA	Lieberman Lab	N/A
Ec ClpX	Lieberman Lab	N/A
Ec ClpS	Lieberman Lab	N/A
Ec ClpB	Lieberman Lab	N/A
Ec GltX	Lieberman Lab	N/A
Ec HisRS	Lieberman Lab	N/A
Ec LysRS	Lieberman Lab	N/A
Ec MetRS	Lieberman Lab	N/A
Ec TyrRS	Lieberman Lab	N/A
Ec ProRS	Lieberman Lab	N/A
Ec LeuRS	Lieberman Lab	N/A
LmLysRS	Lieberman Lab	N/A
Critical Commercial Assays		
HPLC by electrospray ionization and LTQ linear ion-trap mass spectrometry	Taplin Biological Mass Spectrometry Facility	N/A
2-D clean up kit	GE Lifesciences	N/A
SilverQuest kit	Invitrogen	N/A
S30 T7 High-Yield Protein Expression kit	Promega	N/A
Dual-Luciferase reporter assay system	Promega	N/A
Agilent 2200 bioanalyzer	HMS Biopolymer core facility	N/A
Experimental Models: Cell Lines		
YT-Indy	Z. Brahmi (Indiana U.)	N/A
293T	ATCC	N/A
Recombinant DNA		
GFP-6His-ssrA	Tania Baker (MIT)	N/A
Software and Algorithms		
RedFin	Ludesi	N/A
MS-Excel	Microsoft	N/A
MATLAB	Mathworks	N/A
KEGG metabolic map viewer	KEGG	N/A
Pathway Tools	Biocyc	https://biocyc.org/
Uniprot	N/A	N/A
Microbes Online	N/A	N/A

CONTACT FOR REAGENT AND RESOURCE SHARING

Further information and requests for resources and reagents should be directed and will be fulfilled by the Lead Contact, Judy Lieberman (judy.lieberman@childrens.harvard.edu).

EXPERIMENTAL MODEL AND SUBJECT DETAILS

Bacteria

E. coli (Ec) BL21DE3 strain (New England Biolabs), *L. monocytogenes* (Lm) 10403S strain (Walch et al., 2014), *Mycobacterium smegmatis* (Trevisan strain) Lehmann and Neumann (ATCC) and lysate from *M. tuberculosis* (MTB) H37Rv stain (BEI Resources)

were used. Ec *clpX*- strain was a gift of Tania Baker (MIT, Cambridge). Ec *clpP*- and *clpXP*- strains were gifts of Alfred Goldberg (HMS, Boston). Ec, Lm and Ms were grown at 37°C in 2.5% LB, BHI or Middlebrook 7H10 with OADC media, respectively.

METHODS DETAILS

Bacterial plasmids

Putative GzmB substrates were cloned into pET21a (Addgene) and His-tagged proteins were expressed in Ec and purified on a nickel column. The ssrA-GFP plasmid was a gift of Tania Baker (MIT, Cambridge).

GzmB and GNLY

GNLY (a mixture of 15-kDa and active 9-kDa isoforms) and GzmB were purified from YT-Indy, a human natural killer cell line (obtained from Z. Brahmi, Indiana University School of Medicine) (Thiery et al., 2010). Recombinant human inactive serine-to-alanine (S-A) active site mutants were produced in 293T cells (ATCC) as previously described (Dotiwala et al., 2015). Purified recombinant mouse GzmB, expressed in a baculovirus expression system, was purchased from Sigma. Activity of recombinant GzmB was assessed by cleavage of the peptide substrate benzyloxycarbonyl AlaAlaAsp-thiobenzyl ester. For each batch of purified protein, the sublytic concentration of GNLY was determined for each bacterial species, as the concentration that led to a 10%–20% reduction in CFU after 30–60 min of treatment. Because the sublytic concentration varies between batches, it was determined for each protein preparation.

2D-Proteomics

Cell free lysates from Ec, Lm and MTB were treated with 200 nM GzmB or inactive S-A GzmB for 30 min and the proteins prepared for isoelectric focusing (IEF) using the 2-D clean up kit (GE Healthcare Life Sciences). Protein samples were dissolved in 4% CHAPS, 5 M urea, 2 M thiourea and adsorbed onto IEF strips (Bio-Rad). After IEF, the strips were equilibrated in 2% DTT and 2.5% iodoacetamide to reduce and alkylate cysteines and the second dimension was run on a 12% SDS-PAGE gel. Gels were silver stained using SilverQuest kit (Invitrogen), scanned and compared using Redfin software (Ludesi). Spots that disappeared after GzmB treatment were excised from the S-A GzmB-treated sample gel, trypsin-digested in gel, and then analyzed on a nanoscale reverse-phase HPLC by electrospray ionization and LTQ linear ion-trap mass spectrometry at the Taplin Biological Mass Spectrometry Facility, Harvard Medical School. Results from mass spectrometry were checked by comparing the molecular weight and pI of the protein hits to that to the corresponding spots on the gel. Protein targets that returned at least 4, 3 and 12 unique peptides for Ec, Lm and MTB, respectively, were identified as potential GzmB substrates.

Bioinformatics analysis

Genome annotation and COG assignment of putative GzmB substrates for all three species were obtained using the Uniprot and Microbes Online databases (Dehal et al., 2010; UniProt Consortium, 2015). 273 of 278 Ec target genes, 152 of 163 Lm targets, 306 of 334 MTB targets were mapped onto COG categories. Pathway enrichment for the common targets was done using annotation from the KEGG database for Ec (Kanehisa et al., 2014). GzmB target names were mapped on to KEGG Orthology (KO) identifiers prior to visualization on the universal KEGG metabolic map viewer.

Metabolic network modeling

Metabolic genes required for optimal growth were determined using flux balance analysis (FBA) (Orth et al., 2010). FBA is a metabolic modeling approach that identifies a metabolic flux state that satisfies stoichiometric and thermodynamic constraints, while maximizing the flux through a biomass synthesis reaction that represents the synthesis of amino acids, nucleotides, lipids and other essential cellular components. A gene is predicted to impact growth by FBA if a reduction (> 1%) in biomass synthesis is observed after all the metabolic reactions that are associated with a gene are constrained to have zero flux. The 125 metabolic conditions used for identifying metabolic genes necessary for optimal growth were obtained from Chandrasekaran and Price (2010) and are listed in Table S4. Overall, 217 genes, corresponding to 209 COGs were identified to be necessary for optimal growth in over 90% of the conditions. The significance of the overlap between these 209 COGs and 132 GzmB targets was estimated using the hypergeometric test.

GzmB cleavage assay

Bacterial genes, expressed from pET21a with a C-terminal His_6 tag in BL21-DE3 Ec grown in Luria broth, were induced with 0.1 mM isopropyl β-D-1-thiogalactopyranoside (IPTG, Sigma) for 1 hr. The tagged proteins were purified using Ni-NTA Superflow beads (QIAGEN). Purified proteins were diluted 1:100 in 20 mM NaCl, 10 mM TrisHCl, pH 7.5, before adding GzmB at the indicated concentration. To assess intracellular cleavage, GzmB and sublytic GNLY were added to Ec expressing His-tagged aaRS that were induced for 30 min at 37°C with 0.1 mM IPTG, in 50 mM NaCl, 10 mM TrisHCl, pH 7.4. Reactions were stopped after 30 min by boiling in SDS-PAGE loading buffer. Samples were analyzed by immunoblot using anti-His_6 mouse monoclonal Ab (Covance, MMS-156P). As a loading control, blots were probed for cytochrome C (Abcam, ab18738).

In vivo global protein synthesis assay

Bacteria were grown exponentially at 37°C to an optical density at 660 nm of 0.5 to 0.6. 10^6 bacteria were treated with 100 nM GzmB and sublytic GNLY at 37°C in hypotonic buffer (one third deionized water, two thirds HBSS) in the presence of 10 mM N-acetyl cysteine for indicated times. Following treatment, bacteria were either diluted in LB and plated on LB (Ec), BHI (Lm) or Middlebrook 7H10 with OADC (Ms) agar plates to determine CFU or were centrifuged and suspended in M9 (Ec), HTM (Lm) or Hartmans-de Bont (Ms) medium with 10 μCi/ml of [^{35}S] methionine (PerkinElmer) for 1 hr. An equal volume of 25% trichloroacetic acid was added to the samples, which were kept on ice for 30 min. After centrifugation at 10,000 xg at 4°C for 10 min, the protein pellets were dissolved in 100 μl 2% SDS. Samples were counted in a Topcount NXT scintillation counter (PerkinElmer) after adding 300 μl of scintillation cocktail (MicroScint-40). Treatment with chloramphenicol (200 μg/ml) and rifampicin (50 μg/ml) were used as translation and transcription inhibitor controls, respectively.

In vitro transcription coupled translation assay

The S30 T7 High-Yield Protein Expression kit (Promega, WI, USA) was used as an Ec extract-based cell-free in vitro transcription coupled translation system (IVTT). The kit includes extracts that contain T7 RNA polymerase for transcription and all necessary components for translation. The T7 S30 extract mix was pretreated with indicated concentrations of GzmB for indicated times at 37°C. Reactions were terminated by adding 250 μM 3, 4-dichloroisocoumarin (DCI) for 15 min at 37°C. IVTT reactions, started by adding 10 ng of S30 T7-*Renilla* luciferase control plasmid, were incubated at 37°C for 1 hr with constant shaking. Reactions were stopped by placing the tubes at 4°C for 5 min, before measuring luciferase activity by Dual-Luciferase® reporter assay system (Promega).

Ribosome fractionation and treatment

Ec crude ribosomal fraction and ribosomal subunits were isolated as described (Rivera et al., 2015). Briefly, 2 L of exponential bacterial cultures were pelleted and suspended in lysis buffer (10 mM TrisHCl, pH 7.5, 1 mM EDTA, 100 mM NaCl, 250 U/μl lysozyme). Bacterial cells were lysed by glass beating and repeated freeze thaw cycles. Cell debris was separated by centrifugation at 32,000 xg for 60 min, and the supernatant was centrifuged at 70,000 xg for 17 hr. The crude ribosomal pellet was resuspended in association buffer (20 mM HEPES, pH 7.6, 6 mM $MgCl_2$ 30 mM NH_4Cl, 3 mM β-mercaptoethanol) and stored at −80°C. To purify ribosomal subunits, the crude ribosomal fraction was suspended in either association or dissociation (20 mM HEPES, pH 7.6, 1 mM $MgCl_2$ 200 mM NH_4Cl, 3 mM β-mercaptoethanol) buffer and separated on a 10%–50% (w/v) sucrose gradient at 28,000 rpm (Beckman SW28 rotor). Peaks corresponding to 70S, 50S, 30S ribosomal subunits were pooled and concentrated by ultracentrifugation at 70,000 xg for 18 hr. Ribosomal fractions (500 μg in 300 μL association buffer) were treated with indicated concentrations of GzmB for 30 min at 37°C and then separated on a 10%–50% (w/v) sucrose gradient by centrifugation at 24,000 rpm (Beckman SW55Ti rotor) for 16 hr. Ribosome content of fractions was assessed by measuring O.D. at 260 nm.

Transmission electron microscopy

S30 T7 plasmid expressing *Renilla* luciferase was added to Ec cell-free lysate to induce poly-ribosome formation. The translation reaction was terminated by adding chloramphenicol (0.01 mg/ml final concentration). The reaction mixture was clarified (12,000 g, 10 min) and separated on a 2 mL Sephacryl S-500 HR column equilibrated with buffer A (25 mM HEPES, pH 7.6, 500 mM KOAc, 5 mM $Mg(OAc)_2$, 2 mM DTT, 0.01 mg/ml chloramphenicol) at 4°C. Fractions containing polyribosomes were pooled and treated with GzmB for 30 min at 37°C. Treated polyribosomes (5 μl) was applied to an EM grid and negatively stained for 5 min with 2% uranyl acetate. Grids were dried overnight and observed using a JEOL 1200EX transmission electron microscope equipped with an AMT 2k CCD camera.

Ribosome substrate identification by tandem mass spectrometry

Proteins were precipitated from purified Ec ribosomes that were treated with 200 nM GzmB or S-A GzmB for 30 min using the 2-D clean up kit (GE Healthcare Life Sciences). The protein pellets were sent to the Taplin Mass Spectrometry Facility (Harvard Medical School) for terminal amine isotope labeling of substrates (TAILS) analysis. After proteins in each sample were labeled with different tandem mass tags (TMT), the samples were pooled, trypsin digested and analyzed by MS/MS (Kleifeld et al., 2011; Thompson et al., 2003). Primary amines (N-termini, Lys and GzmB cleavage sites) are tagged by TMTs. While amounts of N-termini and internal Lys are the same in both samples, de novo N-termini created by GzmB cleavage are only labeled in GzmB-treated samples.

tRNA synthetase activity assay

Aminoacylation assays were performed as previously described (Cestari and Stuart, 2013). Briefly, recombinant Ec aaRS were pretreated with 100 nM GzmB for 30 min at 37°C. Reactions were terminated by adding 250 μM DCI for 15 min at 37°C. Aminoacylation reactions were performed in 50 μL with GzmB-treated aaRS (40 μg/ml), specific L-amino acid (2 mM), 8 μM Ec tRNA mixture (Sigma), 2 U/ml inorganic pyrophosphatase (PPase, Sigma), 100 μM ATP, and 1 mM DTT in aminoacylation buffer (30 mM HEPES, 140 mM NaCl, 30 mM KCl, 40 mM $MgCl_2$). Reactions were incubated at 37°C for 1 hr and stopped by adding100 μL malachite green (Echelon Biosciences, K-1501) and developed for 30 min at RT. Absorbance at 620 nm was measured using a Biotek Synergy 2 plate reader.

ClpX unfoldase activity assay

Unfolding of purified His-tagged GFP-ssrA was assessed as described (Singh et al., 2000). Recombinant His-tagged ClpX (500 nM), pretreated with 100 nM GzmB or PBS for indicated times, was added to 1.5 μM GFP-ssrA and 2 mM ATP. Fluorescence at 509 nm was recorded every minute after adding ATP, using a Synergy H4 Hybrid Multi-Mode Microplate Reader. Reactions were carried out at 37°C in 50 mM Tris·HCl, pH 7.5, 0.2 M KCl, 30 mM $MgCl_2$, 10% glycerol.

In vivo Clp activity assay

GzmB (100 nM) and sublytic GNLY (20 nM for this strain) were added at 37°C in hypotonic buffer (one third deionized water, two thirds HBSS) to 10^7 exponential phase Ec ectopically expressing GFP-ssrA for indicated times. After washing for 10 min in HBSS, bacteria were fixed with 2% formalin and stained with 4',6-diamidino-2-phenylindole (DAPI) and FM4-64 (Molecular Probes) for 30 min on ice. Stained bacteria were mounted on glass slides using VINOL mounting medium (Sigma) for fluorescence microscopy using an inverted, fully motorized Axio Observer spinning disk microscope. Images were analyzed with SlideBook V5.0 software. Bacterial cell masks were assigned based on FM4-64 fluorescence, and GFP-ssrA fluorescence within the mask for each bacterium was measured to obtain mean fluorescence intensity/cell in at least 15 fields/slide.

GFP refolding by Trigger Factor

The activity of purified His-tagged Ec, Lm and MTB Trigger Factor (TF) was assayed using a protocol adapted from (Singh et al., 2000). GFP-ssrA (30 μM) was denatured by adding 10 M guanidine hydrochloride (GdnHCl) drop wise until all observable fluorescence was lost. TF (500 nM), pretreated or not with 100 nM GzmB for indicated times, was added to 1.5 μM denatured GFP-ssrA at 37°C in 50 mM Tris HCl, pH 7.5, 0.2 M KCl, 30 mM $MgCl_2$, 10% glycerol. The final concentration of GdnHCl were diluted 10-fold in the working sample. GFP fluorescence at 509 nm was measured every minute after adding denatured GFP-ssrA.

Bacterial resistance assay

HBSS, sublytic GNLY (20 nM for this strain), GzmB (100 nM) or both were added at 37°C in hypotonic buffer to 10^7 exponential phase Ec for 30 min. After diluting in hypotonic buffer, Ec were plated on LB agar and incubated overnight at 37°C to determine survival by CFU. A surviving colony from the combined treatment was picked at random, grown to exponential phase in LB, and the procedure was repeated.

Statistical Analysis

Analysis of cell viability and biochemical data was performed using Excel version 1609 (Microsoft, USA). Comparisons of groups were performed using Student's t test and one-way ANOVA test. Statistical significance of the overlap among GzmB targets was performed using the hypergeometric test. In addition, we simulated the effect of a random protease by choosing targets drawn from each species' genome with the same number as the original GzmB targets in each species. We then compared the overlap among this random set of targets with the actual overlap between all three species. We repeated this analysis 500 times and found that the expected overlap between randomly chosen targets was significantly lower than the observed overlap among GzmB targets (p value = 10^{-33}, t test). To determine if the observed overlap between GzmB targets were biased due to protein abundance, we repeated the analysis by using the 500 most abundant proteins in each species from the Protein Abundance Database (Wang et al., 2012). The overlap among random set of targets drawn from this set of abundant proteins was once again significantly lower than the observed overlap among GzmB targets (p value = 10^{-9}, t test). Pathway enrichment analysis, common pathway analysis and KEGG pathways enriched for common orthologs were analyzed and p values determined using a hypergeometric test in MATLAB (MathWorks, USA). A p value cut-off of 0.05 was considered statistically significant.

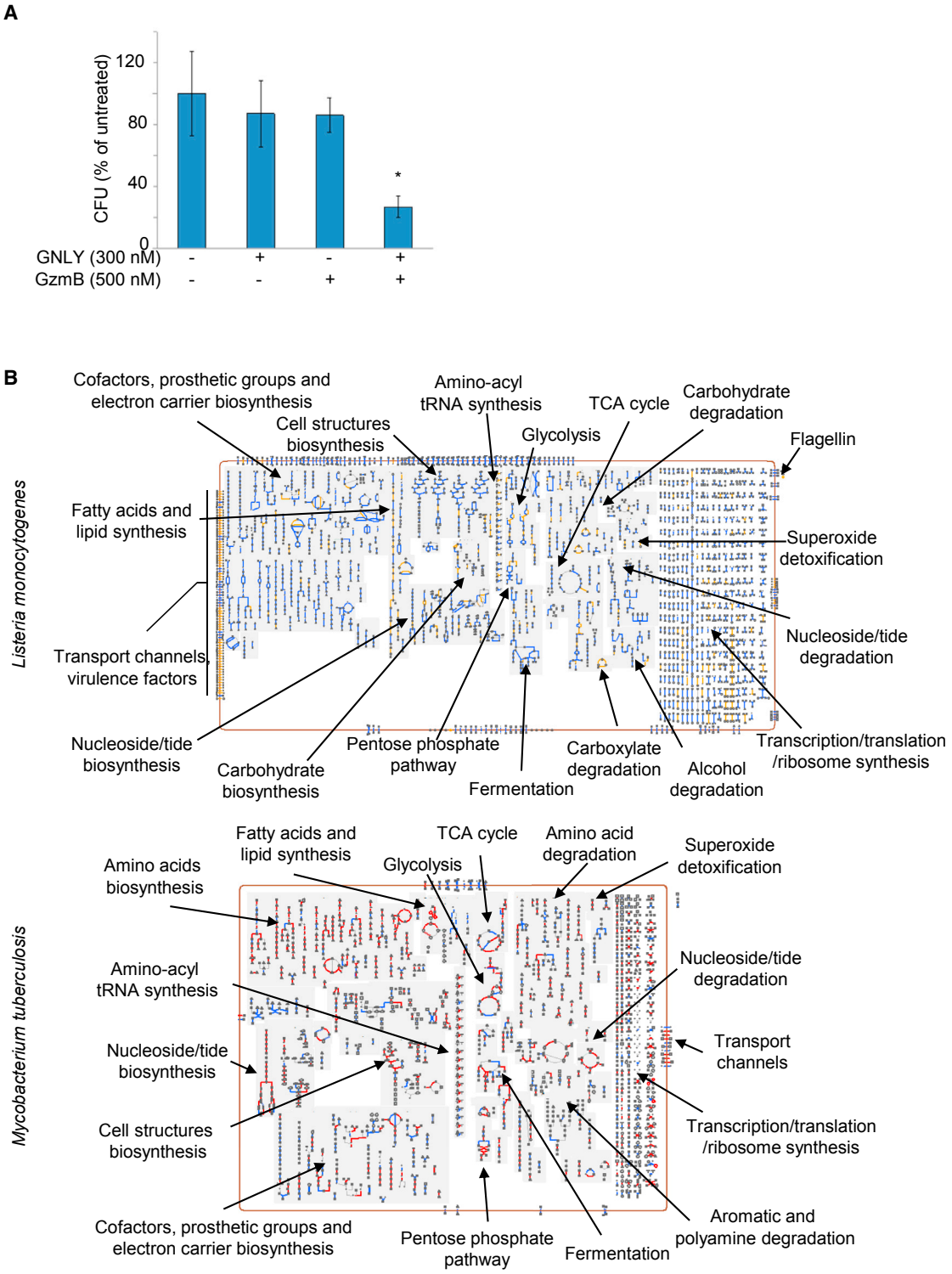

Figure S1. GzmB Substrates in *L. monocytogenes* and *M. tuberculosis*, Related to Figure 1

(A) *M. smegmatis* is killed by sublytic GNLY (300 nM) and 500 nM GzmB. Bacteria treated with GzmB or GNLY alone were not killed. Mean ± SEM of three independent experiments (*$p < 0.05$, Student's t test compared to untreated sample).

(B) Protein targets of GzmB identified by proteomics in Lm (top, orange) and MTB (bottom, red) are viewed using the Bio-Cyc Pathways tools omics viewer. GzmB targets translation, transcription and DNA repair as well as key metabolic pathways in energy, amino acid, lipid, nucleotide and redox metabolism that are central to cell survival.

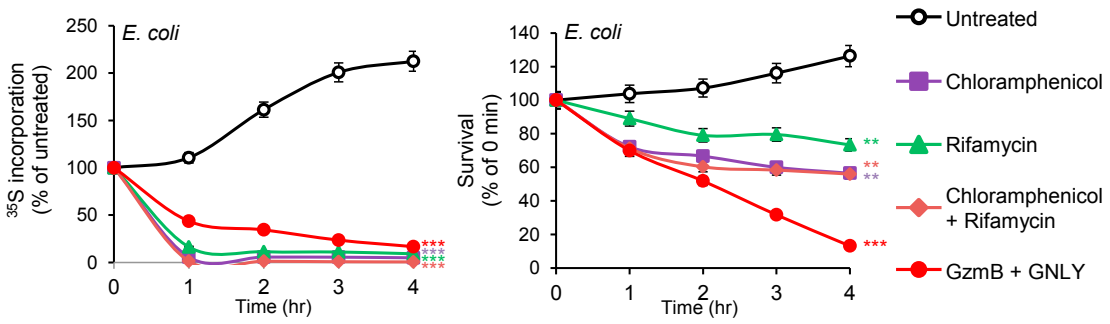

Figure S2. GzmB Disruption of Protein Synthesis Precedes Bacterial Death, Related to Figure 3

GzmB (100 nM) and GNLY treatment of Ec in the presence of a superoxide scavenger decreases ^{35}S incorporation (left) comparably to rifamycin or chloramphenicol treatment. While rifamycin and chloramphenicol are bacteriostatic, GzmB-treated bacteria do not survive treatment. Mean ± SEM of three independent experiments (***$p < 0.001$; **$p < 0.01$, one-way ANOVA compared to untreated bacteria).

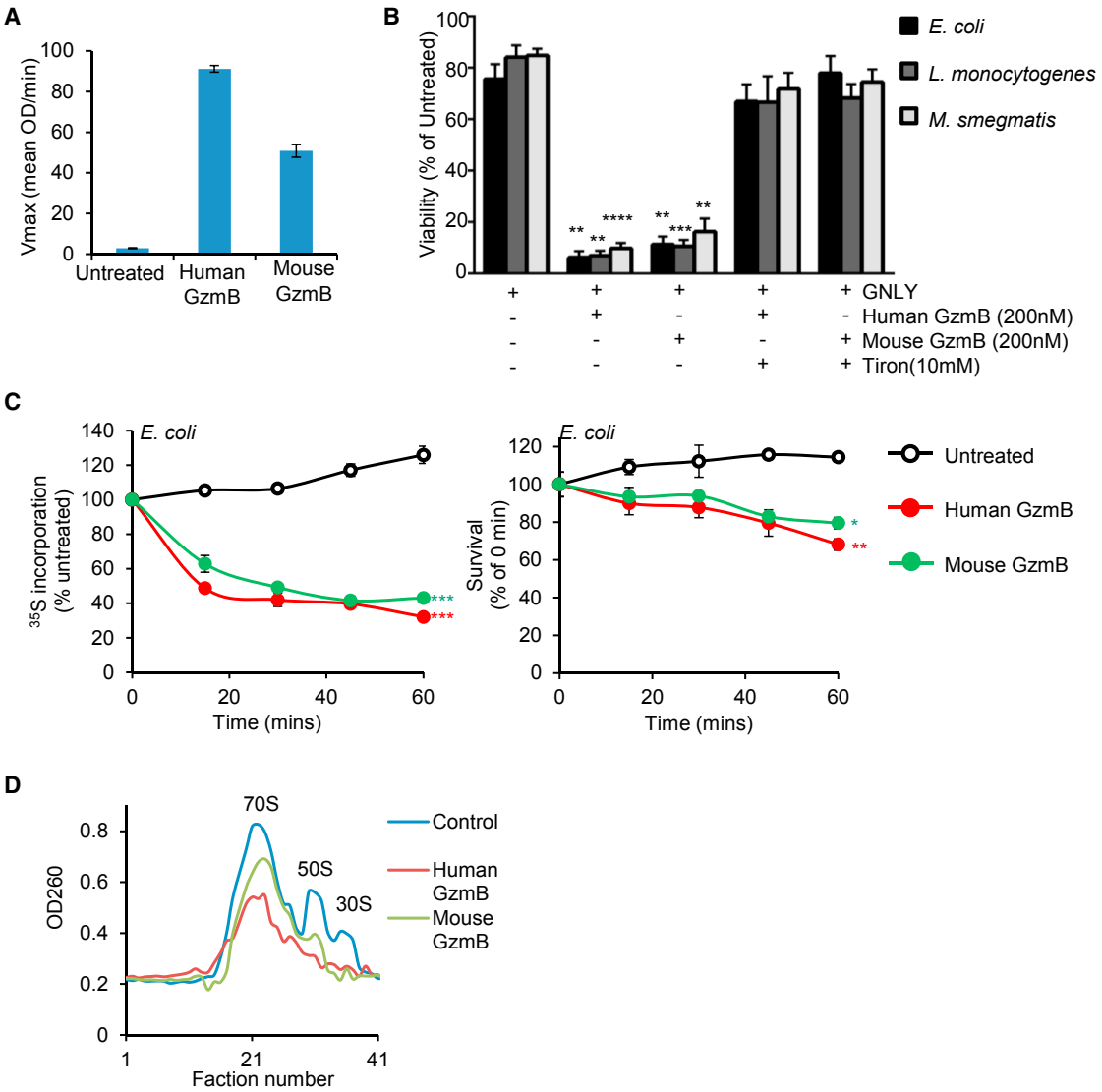

Figure S3. Mouse GzmB Kills Bacteria, Inhibits Protein Synthesis, and Disrupts Ribosomes, Related to Figures 3 and 4

(A) Activity of human and mouse GzmB was determined by the maximum rate of hydrolysis of the Boc-Ala-Ala-Asp-S-Bzl peptide substrate. Data depict a representative experiment performed in triplicate (n > 3).

(B) Ec, Lm and Ms were treated with 200 nM human or mouse GzmB and sublytic (20 nM) GNLY for 20 min in the presence or absence of 10 mM Tiron and surviving bacteria were assessed by CFU assay. Mean ± SEM of three independent experiments (****p < 0.0001; ***p < 0.001; **p < 0.01; Student's t test, compared to untreated).

(C) GNLY and human or mouse GzmB treatment of Ec leads to rapid loss of ^{35}S incorporation (left) before loss of viability (right). The reactions were performed in the presence of an ROS scavenger to inhibit the rapid oxidative death caused by GzmB and GNLY. Mean ± SEM of three independent experiments (***p < 0.001; **p < 0.01; *p < 0.05, one-way ANOVA compared to untreated bacteria).

(D) Sucrose gradient fractionation of Ec crude ribosomal fraction after incubation with or without human or mouse GzmB for 30 min. The concentrations of mouse and human GzmB (540 nM and 300 nM, respectively) were chosen to have equivalent enzymatic activity as measured in (A). The absorbance at 260 nm measures the RNA content of each ribosomal fraction.

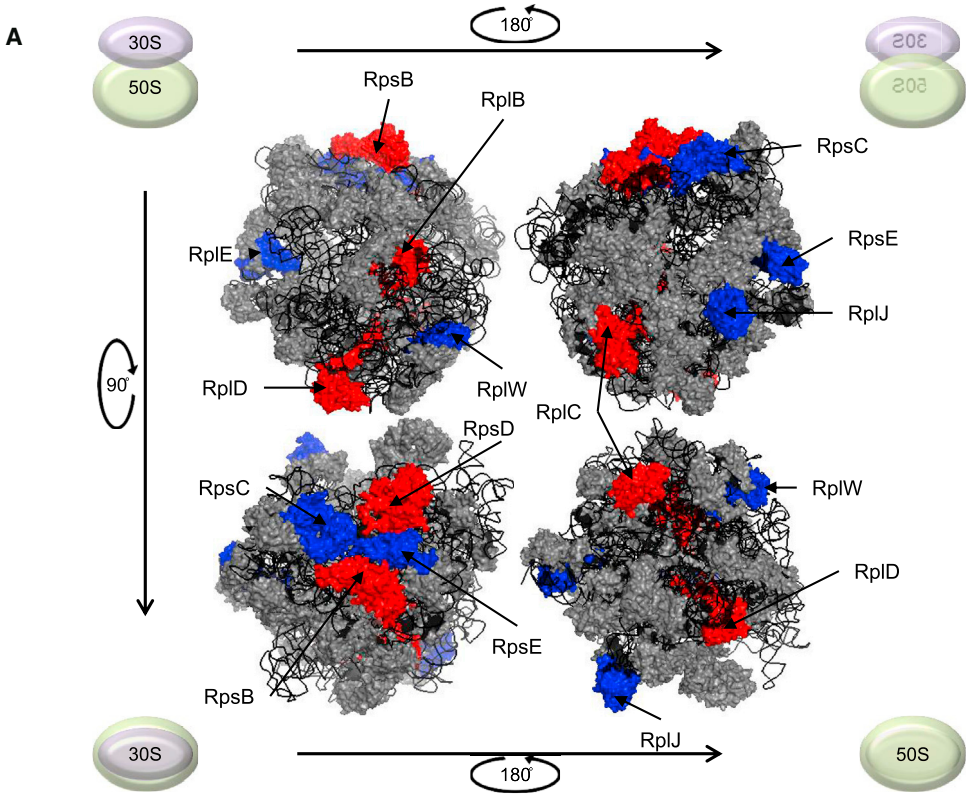

B

RpsJ	RplC	RplD	RplW	RplB	RpsS	RplV	RpsC	RplP	RpmC	
sra	RplC	RplD	RplU	L8e	RpsO	RplQ	RpsC	RplJ	RpmI	
RpsQ	RplN	RplX	RplO	RplE	RpsN	RpsH	RplF	RpsO	RpmD	RplR	RpsE
RplN	RpmJ	RpsM	RpsK	RpsD	RpsN	RplR	RplQ	RplM	RpsP	RpsI	
RpsG	RpsL	RpmD	RplL	RplJ	RplA	RplK					
RpmB	RpmG	RplU	RpmA	RpsP	RplS	RpsA	RpsT	RpsU	RplY		
RpsA	SAe	RpsO	RpmI	RplT	RpmH	RpsM	RpmE	RpmF	RplI	RpsR	RpsF

Unique to *E. coli*

Unique to *M. tuberculosis*

Unique to *L. monocytogenes*

Shared by at least 2 species

Figure S4. Ribosomal Protein Targets of GzmB, Related to Figure 4

(A) GzmB substrates, identified by proteomics, shared by at least 2 of the 3 studied bacterial species (Red) or unique to Lm (Blue) are shown using Ec ribosome structure 5KPX deposited in PDB (http://www.rcsb.org/pdb/explore.do?structureId=5kpx).

(B) GzmB substrates, identified by proteomics, overlaid onto ribosome protein encoding operons in the universal KEGG map. Proteins in both the large and small subunit of the ribosome are predicted substrates. All Ec and MTB predicted substrates are predicted substrates in at least one other species.

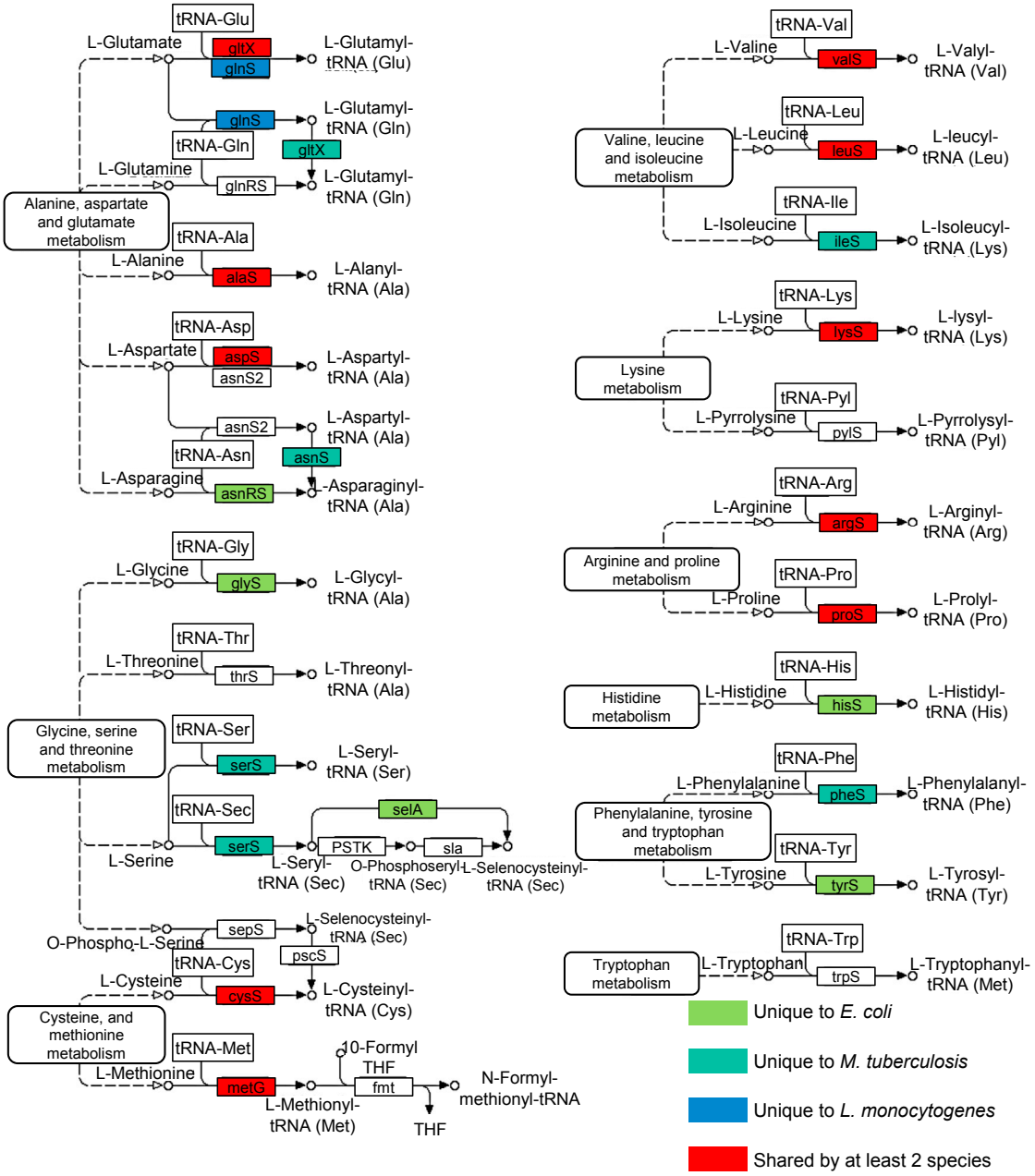

Figure S5. Aminoacyl tRNA Synthetases Predicted by Proteomics to Be Cleaved by GzmB, Related to Figure 5

Aminoacyl tRNA synthetases (aaRS) targeted by GzmB in Ec, Lm and MTB. Many predicted aaRS substrates were identified in at least 2 bacterial species.

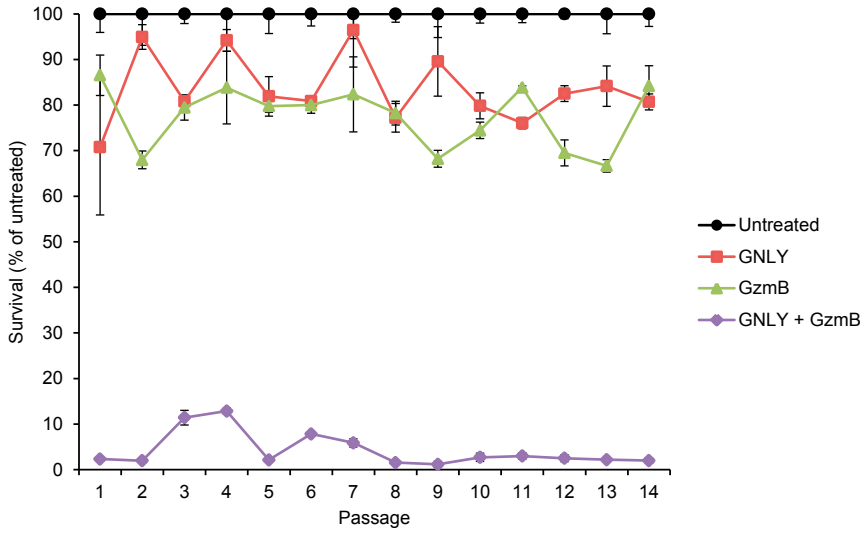

Figure S6. ***E. coli*** **Do Not Become Resistant to Sublytic GNLY and GzmB after Repeated Exposures, Related to Figure 3A**

Ec were treated with 20 nM GNLY, 200 nM GzmB or both for 30 min and plated to assess CFU. At least one surviving colony was retreated. Serial passaging was continued for 14 cycles without development of resistance. Shown are mean ± s.d of three independent experiments.